Doctoral Dissertations

Student Theses and Dissertations

1970

Structures and relationships of some Perovskite-type compounds

Christian Michel

STRUCTURES AND RELATIONSHIPS OF

SOME PEROVSKITE-TYPE COMPOUNDS

by

Christian *Gabriel* Michel, 1939-

A DISSERTATION

Presented to the Faculty of the Graduate School of the

UNIVERSITY OF MISSOURI - ROLLA

In Partial Fulfillment of the Requirements for the Degree

DOCTOR OF PHILOSOPHY

in

PHYSICS

1970

ABSTRACT

A model for crystallographic transitions in perovskites is proposed. The model consists of regular octahedra sharing corners and topologically able to rotate without distortion around their three-fold axes. This model, with $R\bar{3}c$ symmetry (18e position) can be described in terms of a continuous rotation of angle, ω , of octahedra from two ideal symmetry forms: the hexagonal close-packed and the cubic face-centered configurations. A parametric relation is derived between ω and the rhombohedral cell angle, α , or the corresponding hexagonal axial ratio c/a. A wide range of atomic structures based on a framework of regular or slightly distorted octahedra sharing corners can be derived from this model. A number of compounds of composition ABX_3 are examined. In all of these the anion X lies exactly or approximately in 18e position of the $R\bar{3}c$ space group with the cation B midway between the AX_3 layers. The site of the cation A may be vacant, as in the case where X is fluorine.

These pseudosymmetric compounds can be viewed also as being generated by an array of linear chains of rigid octahedra sharing corners. Along this chain, ϕ , the bond angle (cation B - anion X - cation B) is related to the bimolecular rhombohedral cell angle, α , or equivalently, to the variable parameter, x , of the anions $[x, 0, 1/4]$,

(hexagonal set, $R\bar{3}c$.) These theoretical relationships are compared graphically to some crystallographic data for a trifluoride-type series, BF_3, (B = Ru, Co, V, Fe, Ti) and a perovskite-type series, ABO_3, (A = Bi, Pb, La, Li, and B = Fe, Zr-Ti, Co, Al, Nb, Ta). The experimental data for all of these compounds are in excellent agreement with the theoretical relationships. The atomic positions of the perovskite-type compounds $PbZr_{0.9}Ti_{0.1}O_3$ and $BiFeO_3$ were determined using X-ray and neutron diffraction. Their octahedral framework can be considered as an early stage of a continuous trigonal rotation which is fully developed in $LiNbO_3$ and $LiTaO_3$. In this isomorphous ferroelectric series, the B cation shifts from the ideal perovskite positions and are related to the A cation shifts and the spontaneous polarization. The symmetry is then reduced to the non-centrosymmetric space group, R3c. In all of these compounds the distortion of the octahedra is a second order effect compared to the trigonal rotation. Such deformations, in agreement with the theoretical data, generate superstructure reflections which depend only on the oxygen position, and the intensity of these reflections can be correlated with the trigonal rotation, ω. The temperature dependence of ω for the low temperature phase of $PbZr_{0.9}Ti_{0.1}O_3$ is consistent with the existence of an unstable phonon mode at the ($\frac{1}{2}\frac{1}{2}\frac{1}{2}$) point at the Brillouin zone corner, as in $LaAlO_3$. One of the most significant

aspects of this work has been to relate certain phase transitions in ferroelectric materials, such as $PbZr_{0.9}Ti_{0.1}O_3$, with intensively studied transitions in some non-ferroelectric perovskites, such as $LaAlO_3$ and $SrTiO_3$.

ACKNOWLEDGEMENTS

TABLE OF CONTENTS

LIST OF TABLES

LIST OF FIGURES

I. INTRODUCTION

Compounds with the chemical formula ABX_3 form an extensive class of structurally related materials in which the large A cation has a radius between 1.0 and 1.9 Å, while the B cation's radius is between 0.5 and 1.2 Å. In this formula, X is an anion such as oxygen, sulfur, fluorine, or chlorine. The related structures of this class can all be described by a close-packed AX_3 layer, the B cations filling all anion octahedral sites between these layers. In this wide range of compounds, the atomic structure is based on a framework of octahedra linked at their corners.

These octahedra are either regular or approximately so in size and shape. As a result, this framework can be considered as an atomic array of rigid units.

In this work, a geometrical study is made of a model of regular octahedra, sharing corners and topologically able to rotate without distortions around their three-fold axes. This model is in fact the basic framework of the pseudo-symmetric compounds largely investigated in the last decade which belong to the perovskite family.

The theoretical and experimental study of such pseudo-symmetric compounds is of considerable interest due to the unusual physical properties, often related to small atomic displacements from a higher symmetry form.

Our first purpose is to examine the departure from cubic symmetry of the rhombohedral compounds ABO_3 (A = Bi, Pb, La, Li, and B = Fe, Zr-Ti, Co, Al, Nb, Ta) and BF_3 (B = Mo, Ta, Nb, Ru, V, Fe, Co, Rh, Ir, Pd, Ti). In all of these compounds, the type of distortion of the anion framework is the same.

The magnitude of this distortion can be evaluated by either the angle α of the rhombohedral unit cell containing two formula units or the corresponding axial ratio, c/a, in the hexagonal cell. The theoretical part of this work is to establish and discuss how the atomic positions are correlated with the unit cell dimensions. These considerations are then applied to the structures of the perovskite ferroelectric compounds, $BiFeO_3$ and $Pb(Zr-Ti)O_3$, in the rhombohedral phase. In spite of the many previous studies of these compounds, the structures were not understood until the completion of this work.

A considerable effort has been made recently in applied research on the perovskite compounds with both ferroelectric and magnetic properties. These compounds could be important in electronic microcircuit technology.

$BiFeO_3$ is an example of a compound which is ferroelectric and antiferromagnetic with a weak ferromagnetic moment.

Any explanation of the ferroelectricity, magnetism and phase transitions of these substances must begin with

a correct knowledge of their structures. To arrive at an understanding of the structures and their related physical and chemical properties, a systematic study, by means of neutron and x-ray diffraction on single crystal and poly-crystalline pure samples, was made. This constituted the experimental part of this work.

II. LITERATURE REVIEW

A. The ABX₃ Perovskite-type Compounds

In the compounds considered with the chemical formula ABX_3, X is supposed to be an anion, such as oxygen or fluorine, and A, B are the cations. The structure of these materials can be described by a stacking of ordered close-packed AX_3 layers, the B cations filling all anion octahedral sites between these layers. The two types of ideal AX_3 layer stacking are the cubic and the hexagonal. In the ideal cubic packing, the BX_6 octahedra share corners in three dimensions to form the cubic perovskite structure.[1] The perovskite family also includes all of the compounds with structures which can be derived from the ideal perovskite type by small lattice distortions or omission of some atoms. In these perovskite-type compounds, A is a monovalent, divalent, or trivalent element and B is respectively pentavalent, tetravelent, or trivalent.

The structures and the physical properties of these perovskite-type compounds have received much study.[2,3,4] The compounds are characterized by the rather small size of the B cation compared to the A cation. The linear chains of BX_6 octahedra are extended along every [100] direction. The highest symmetry form of these perovskites then belongs to the ideal cubic structure in the centrosymmetric holohedral space group Pm3m. In this case, the

coordinates of the atoms are:

A   (000)

B   ($\frac{1}{2}\frac{1}{2}\frac{1}{2}$)

X   ($\frac{1}{2}\frac{1}{2}0$), ($\frac{1}{2}0\frac{1}{2}$), ($0\frac{1}{2}\frac{1}{2}$)

This ideal perovskite structure requires one cation, A, to be capable of coordination number 12, and the other, B, of 6 coordination. Consequently, the cation A must be rather large. If A, like B, can only have coordination 6, an entirely different arrangement is taken up. The compound ilmenite, $FeTiO_3$, is such an example. In other words, the framework of BX_6 octahedra determines the dimensions and the stability of these perovskite-type structures. This stability is characterized by the "tolerance factor", t, which is defined in the following way:

$$R_A + R_X = t\sqrt{2}\ (R_B + R_X)$$

Here, R_A, R_B and R_X are the ionic radii of the A, B and X ions, respectively. The criterion established by Goldsmidt is that when t is exactly equal to unity, the packing is "ideal". When t is greater than one, there is too large a space available for the B ion. In this case, the ion has been visualized as "rattling" inside its octahedron.

B. Electrical Properties

A classification of the perovskite compounds has been made by S. Roth[4] on the basis of ionic radii and polarizibility of the constituent ions. Roth has shown that the role of the various ions in the structure cannot be expressed only by means of their ionic radii. Other factors are very important, such as polarizibility,[5,6] and the character of the bonding[7] must also be taken into account. In addition, the crystal symmetry also plays an important role, especially in any explanation of the electrical properties. It should be noted that no ferroelectric material has been found to date in the subgroup of double fluorides. Hence, the discussion on electrical properties will be limited to the perovskite-type double oxides.

Piezoelectricity may be exhibited only by crystals in 20 non-centrosymmetric point groups. If the crystal has this characteristic, the application of an external force causes a displacement of electric charge. A subgroup of 10 of these 20 piezoelectric groups possesses a polar symmetry and may show ferroelectricity. The definition of ferroelectricity is not completely precise. Unlike piezoelectricity, ferroelectricity cannot be definitely established from a knowledge of the crystal's symmetry, but requires additional dielectric measurements.

The different conditions for the presence of ferroelectrocity in a crystal are discussed at length in the

literature.[8,9,10] According to Megaw,[11] a sufficient condition is that the materials exhibit a hysteresis loop, indicative of reversible spontaneous polarization.[12,13] However, the hysteresis loop of $PbTiO_3$,[14] one of the leading representatives of this class of ferroelectric crystals, has not been demonstrated, and it is accepted as ferroelectric for other reasons.

If the crystal is antiferroelectric, its structure is characterized by antiparallel displacements of certain atoms, the symmetry is non-polar, and the spontaneous polarization cannot be observed. $PbZrO_3$ [15] is generally considered one of the most important representatives of this class of antiferroelectrics, even though it may have a polar axis.

Many of these double oxides of perovskite-type compounds are characterized at a phase transition by a discontinuity of the dielectric constant. Hence, the Curie temperature can be detected by electrical measurements. Above this temperature, the spontaneous polarization is absent and the crystal is in its higher symmetry form. As the crystal's temperature falls through the Curie point, a pseudosymmetric structure transition takes place and its structure becomes distorted to a space group of lower symmetry. Some crystals have more than one pseudosymmetry low temperature form. This is the case for the solid solutions of $Pb(Zr, Ti)O_3$ in the rhombohedral

phase.[16,17,18]

C. The Pseudocubic Distortions

Experimental evidence shows that the perovskite-type structure dominates when the tolerance factor is between 0.8 and 1.1 and the ilmenite-type structure occurs for $t < 0.8$. Megaw[19] has classified the perovskite oxides according to the type of distortion.

1. Distorted small cell perovskite. The unit cell contains only one formula unit with cell edges approximately 4 angstroms in length.

2. Distorted multiple-cell perovskite. Such a cell is made up of a number of the small perovskite cells as subcells. The structure in this cell can be ferroelectric or antiferroelectric. Since the atomic displacements in an antiferroelectric are antiparallel, the translation - repeat unit must contain at least two formula units. The existence of a multiple cell structure in a perovskite is a necessary condition but not sufficient for the occurrence of antiferroelectricity. The shift of the atoms from the ideal in the case of multiple cells is non-equivalent. Consequently, superstructure lines appear on the x-ray and neutron diffraction diagrams. These "extra" reflections occupy positions between those of the cubic pattern. The non-equivalent atomic shift from the ideal is generally very small and the resulting superstructure

reflections are very weak. When the multiple cell arises from the light atom shifts, the superstructures, in many cases, are in doubt or unobserved. As a result, the literature shows many conflicting reports assigning structures or even symmetries to certain materials.

D. Compounds with LaAlO₃ Type Distortion

Generally, in the perovskite compounds, two different kinds of distortion from the ideal structure can be distinguished.

1. A tilt of the oxygen octahedra around the large A cation. The distortion in $LaAlO_3$ is an example extensively studied in the literature.[20] In this particular case, the oxygen octahedra rotate without deformation around their polar axes.

2. A shift of the cations from their ideal perovskite positions. When the B cation is not central, its octahedron is then distorted and becomes irregular.

Both kinds of distortion may occur at once; the distortion of $BiFeO_3$ is an example of oxygen octahedron tilt with a shift of the cations from the ideal perovskite positions. We have recently reported the structure of $BiFeO_3$[21] and $Pb\,Zr_{0.9}\,Ti_{0.1}\,O_3$.[22] The anion framework of these isomorphous compounds can be described[23,24] as generated by a rotation of the oxygen octahedra around the triad axis [111] in the same type of oxygen shift as in

$LaAlO_3$. The cations are shifted along the [111] from the geometrical center of their octahedra. Thus, the resulting space group is non-centric and allows ferroelectricity. The presence of ferroelectricity of $BiFeO_3$, in doubt according to the literature,[25] was recently detected in our laboratory. The octahedral framework rotation is associated with a non-equivalent oxygen shift which causes superstructure reflections. Although missed or in dispute in the previous studies,[26,27] these superstructure reflections were observed without ambiguity in our experimental work on neutron and x-ray single crystal diffraction.

Structurally, $LiNbO_3$[28] and $LiTaO_3$[29] can be considered as isomorphous with $BiFeO_3$ and $Pb(Zr_{0.9}Ti_{0.1})O_3$. However, these lithium double oxides are also closely related to ilmenite ($FeTiO_3$). It was originally believed, in fact, that these compounds were of the ilmenite-type. It was later shown by Bailey[30] that the structure of $LiNbO_3$ is significantly different from that of ilmenite. Both structures were determined with precision recently in the very detailed work of Megaw[31] and Abrahams.[28] The framework is indeed based upon hexagonal close-packing of oxygen ions, while the metal ions are aligned along the rhombohedral [111] direction. The oxygen octahedra share corners as in the case of perovskite-type compounds. Thus, Megaw advanced the suggestion that $LiNbO_3$ may be considered as a very distorted perovskite compound.

A similar idea is developed in this work by assuming the oxygen octahedra as rigid units able to rotate without deformation around their three-fold axes from the ideal perovskite position to the hexagonal close-packed configuration. In such circumstances, other compounds with the same type of oxygen framework as $LaAlO_3$ have to be considered. This kind of deformation is not limited to the perovskite-type compounds. A series of the trifluorides has been found to be related.[32,33,34] The structure of these isomorphous compounds with B = Ru, V, Co, Fe, Ti can be looked upon as a distorted $LaAlO_3$ type anion frameowrk, the B cation remaining unshifted from the center of the fluoride octahedron.

III. THEORETICAL

A. Pseudosymmetric Structures

1. Pseudosymmetric structure considerations. In a
pseudosymmetric structure, the atoms are slightly dis-
placed from positions corresponding to a higher symmetry
form. These displacements are of the order of one-tenth
of the interatomic distances. The best known examples
are to be found in substances which have a pseudo-perov-
skite structure. In these structures, the magnitude of the
atomic displacement varies from 0.05 $\overset{o}{A}$ up to about 0.5 $\overset{o}{A}$
for the highly distorted perovskite-type compounds. From
these distortions there results a loss of symmetry and a
pseudocubic cell. This pseudocubic deformation is gene-
rally evaluated by the c/a parameter ratio or the pseudo-
cubic angle. A splitting of the x-ray diffraction peaks
from the ideal cubic pattern is related to this pseudo-
cubic deformation.[35] The pseudocubic splitting can then
be measured by x-ray powder diffraction, and the resulting
pseudocubic deformation evaluated by the high angle re-
flections. Nevertheless, the symmetry and the magnitude
of this pseudocubic deformation are often difficult to
determine. This difficulty results mainly because two
different displacement configurations may give nearly the
same peak intensities. To resolve the ambiguity, a large
number of accurate intensity measurements is needed. Very

pure powder samples or single crystals of materials being investigated are not always available, and this has been the cause of many discrepancies in the literature. Up to the present, then, only a few pseudosymmetric structures have been resolved in detail.

It should be noted that most of the time the pseudosymmetric structure contains more than one formula unit. In the resulting multiple cell, the distortion is calculated from superstructure reflections, generally very weak, which are of considerable importance because their extinction rules characterize the crystal symmetry, and their intensities, the magnitude of the non-equivalent atomic shift.

2. <u>Superstructure reflections</u>. In a pseudosymmetric structure, the reflections most sensitive to small ionic displacements are the superstructure reflections, which are produced entirely by such displacements. If x_i, y_i, z_i are the parameters of the ith ion in its undisplaced position in the unit cell, expressed as fractions of the cell repeat distances, and δ_i^x, δ_i^y, δ_i^z are the fractional vector displacements , then, putting:

$$\Delta_i = 2\pi (h\delta_i^x + k \delta_i^y + \ell \delta_i^z)$$

$$\theta_i = 2\pi (h x_i + k y_i + \ell z_i)$$

the structure amplitude for reflection (hkℓ) for the unit
cell is given by

$$|F|^2_{hk\ell} = \{\sum_i f_i^{hk\ell} \sin(\theta_i + \Delta_i)\}^2$$

$$+ \{\sum_i f_i^{hk\ell} \cos(\theta_i + \Delta_i)\}^2$$

Expanding this equation, and introducing the approximations
that for δ small $\cos \Delta_i \simeq 1$, $\sin \Delta_i \simeq \Delta_i$ we have,

$$|F|^2_{hk\ell} = \{\sum_i f_i^{hk\ell} \sin\theta_i + \sum_i f_i^{hk\ell} \Delta_i \cos \theta_i\}^2$$

$$+ \{\sum_i f_i^{hk\ell} \cos\theta_i - \sum_i f_i^{hk\ell} \Delta_i \sin\theta_i\}^2$$

Now if the undistorted ideal structure has a center of
symmetry, and the origin is taken at this point,

$$\sum_i f_i \sin\theta_i = 0 \quad ,$$

If superstructure reflection only is considered,

$$\sum_i f_i \cos\theta_i = 0$$

The structure amplitude expression now becomes:

$$|F|^2_{hk\ell} = \{\sum_i f_i^{hk\ell} \Delta_i \sin\theta_i\}^2$$

$$+ \{\sum_i f_i^{hk\ell} \Delta_i \cos\theta_i\}^2 \tag{1}$$

where all θ_i are known. Using this equation, the expressions for the structure amplitude for the various classes of superstructure reflections can be expressed in terms of the atomic displacements.

3. <u>Relationship to some physical properties</u>. The polarization of ionic crystals can consist of two parts. One part, the electronic distribution, arises from the polarization of the electronic distributions of the individual ions. The other part, the ionic polarization, arises from the displacement of the entire ion from the crystal's higher symmetry form. The ferroelectric polarization is determined by the small atomic displacements from the ideal structures. In the perovskite-type structures, the two different kinds of displacements which can be distinguished are the off-center displacement of the cations and the octahedral tilt. These specific distortions and their effect on the electrical properties will be considered separately.

a. <u>The off-center displacement of cations</u>. It appears that in all perovskite-type compounds which show ferroelectricity, the oxygen atoms are strongly bound to

the metal atoms, which are slightly displaced from the geometrical center of an octahedron. The displacement results in a rearrangement of the electron cloud associated with the bonds, and the homopolar bond for this central atom becomes unsymmetrical. This gives rise to a dipole moment of the unit cell characteristic of a ferroelectric.

Studies of the off-center displacement of cations in octahedral environments have been presented in the literature.[36] So far, these considerations have been qualitative and have shown that the displacement must be strongly influenced by polarization. It appears that the B cation shift decreases when the temperature increases. This variation of the off-center effect at different temperatures can be associated with a variation in the homopolar bond system to the atom concerned.

A study by Abrahams[37] of many displacive ferroelectrics in which atomic positions have been determined has shown that a fundamental relationship exists between the displacement, Δz, of the central atom and the Curie temperature. This relation has the form:

$$T_C = 2.10^4 \, (\Delta z)^2 \qquad (2)$$

where Δz is in Angstroms and T_C in absolute units. In addition, the spontaneous polarization, P_s, was found to be related to Δz by the equation:

$$P_s = (258)10^4 \Delta \ z\mu C \ cm^{-2} \qquad\qquad (3)$$

These empirical relationships are applicable to a large
number of ferroelectrics, including the compounds studied
in this work. Nevertheless, further experimental and
theoretical studies are necessary to establish the full
range of validity of these relationships.

b. <u>Anion octahedral tilt</u>. The deformation study
of structures with frameworks of linked octahedra may be
divided into two parts: (a) the tilt of the octahedra
relative to one another, and (b) their individual dis-
tortions.

The distortion of the octahedron is characterized by
the spread of the oxygen distances around the average
value. This distortion is directly associated with the B
off-center cation. The difference, e, between relaxed
and unrelaxed edge lengths of the octahedron has been
found to a first approximation to be linearly correlated
with the magnitude, μ, of the B cation shift. For perov-
skite-type compounds, containing niobium, the relationship
$\mu \simeq 8 \cdot e$ has been established by Megaw.

In the BO_6 octahedron, the B cation is strongly
bound to the oxygens, the octahedron distortion is rela-
tively small, and the octahedron can be considered as a
rigid unit, regular or approximately so. Crystallographic
data on many compounds confirm this and show that the

distortion of the octahedron is a second order effect compared to its tilting. For the highly distorted perovskite compounds, the pseudocubic deformation is only due to the octahedra tilt.

In this study, a particular framework deformation will be considered consisting of octahedra sharing corners and rotating around the cubic triad axis [111]. This model is the basic anion framework of a large range of compounds, the prototype being $LaAlO_3$.

The trigonal rotation of AlO_6 octahedra has been investigated recently by E.P.R., neutron and Raman scattering.[38]

It has been observed that the rotation in several compounds varies quantitatively in the same way, as a function of reduced temperature, and thus, can be considered as an order parameter, characteristic for perovskite compounds. Considerable theoretical attention has been given to the study of the phase transitions in the ' perovskite compounds ABO_3 which involve rotations of the BO_6 octahedra[39,40] as in $LaAlO_3$. These phase transitions are associated with an unstable phonon mode at the corner point [½½½] of the Brillouin zone.[41]

B. **Relationships in a Framework of Regular Octahedra Sharing Corners**

1. Model of regular octahedra sharing corners. A
regular octahedron, projected onto a plane perpendicular
to one of its triad axes, is shown in Fig. 1. Let us
refer its six corners P_k (k = 0 to 5) to a hexagonal sys-
tem $\vec{O}_x$, $\vec{O}_y$, $\vec{O}_z$, providing $\vec{O}_z$ is parallel to the triad
axis Δ, and providing the (x,y) plane perpendicular to
$\vec{O}_z$, is midway between the two opposite faces.

The octahedron edge $\underline{e}$ and the distance $\underline{d}$ between two
opposite faces are related by:

$$\underline{d} = \underline{e} \ \sqrt{2/3} \qquad\qquad (4)$$

The projection ℓ of $\vec{O}P_k$ on the (x,y) plane is $\ell = \dfrac{e}{\sqrt{3}}$.

For the following calculations, the unit vectors $\vec{i}$, $\vec{j}$, $\vec{k}$
along $\vec{O}_x$, $\vec{O}_y$, $\vec{O}_z$ are given as:

$$|\vec{i}| \ = \ |\vec{j}| \ = \ \frac{e}{\sqrt{3}}$$

$$\qquad (5)$$

$$|\vec{k}| \ = \ \frac{e}{\sqrt{6}} \ = \ \frac{d}{2}$$

Then the coordinates of the vector $\vec{O}P_k$ can be expressed
by:

$$\vec{O}P_k = [6]^k \cdot \begin{pmatrix} 1 \\ 0 \\ (-1)^k \end{pmatrix} \qquad \text{with (k = 0,1,...5)}$$

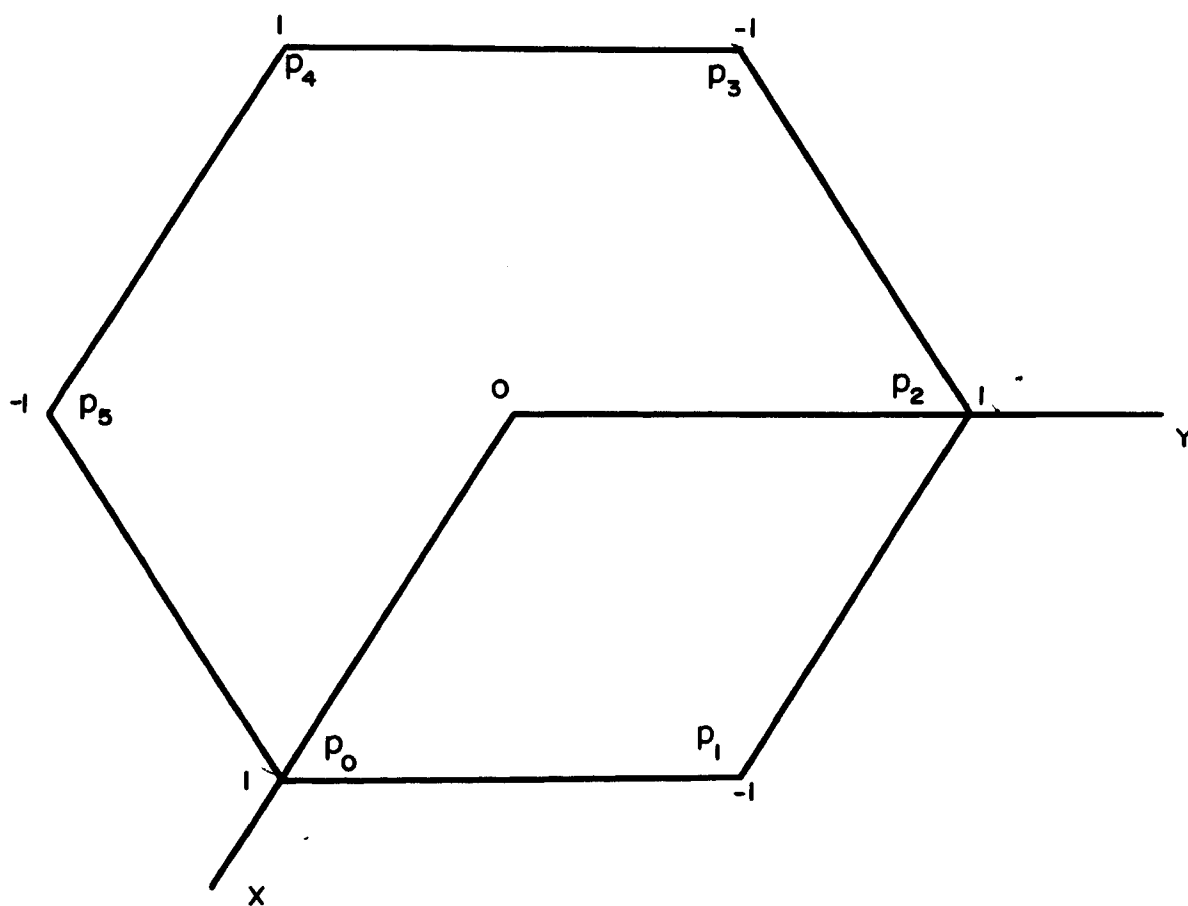where the matrix [6] represents the six-fold rotation

Figure 1. A regular octahedron projected onto a plane perpendicular to one of its triad axes.

$\vec{O}_z$,

$$[6] = \begin{pmatrix} 1 & 1 & 0 \\ 1 & 0 & 0 \\ 0 & 0 & 1 \end{pmatrix}$$

A chain of regular octahedra sharing one corner and labeled as a series ($n = 0,1,2...$) is shown in Fig. 2a. One of the three fold axes Δ_n of each octahedron $\underline{n}$ is parallel to $\vec{O}_z$ in the (x,y) plane; consequently, their geometrical centers O_n lie on a straight line. The O_n coordinates are $\vec{OO}_n = 2n \cdot \begin{pmatrix} 1 \\ 0 \\ 1 \end{pmatrix}$. Then, the six corner coordinates $P_k(n)$ of the octahedron $\underline{n}$ are given by the matrix relation:

$$\vec{OP}_k(n) = [6]^k \cdot \begin{pmatrix} 1 \\ 0 \\ (-1)^k \end{pmatrix} + 2n \begin{pmatrix} 1 \\ 0 \\ 1 \end{pmatrix}$$

Now, from the configuration (Fig. 2a) and assuming all the Δ_n remain parallel in the (xz) plane, a rotation of the reference octahedron, $n = o$, by an angle ω_o around Δ_o gives rise to a rotation $\omega_n = (-1)^n \omega_o$ around Δ_n for the octahedron $\underline{n}$. These rotations lead to the model in Fig. 2b, where the octahedra center coordinates become:

$$\vec{OO}_n = 2n \cdot \begin{pmatrix} \cos \omega \\ 0 \\ 1 \end{pmatrix}$$

Figure 2

(a)   Linear chain of regular octahedra sharing
      one corner and labeled as a series
      $(n = 0, 1, 2...)$.

(b)   Linear chain with a rotation of the reference
      octahedron, $n = 0$, to an angle ω_0 around one
      of its triad axes.

(c)   Configuration of a linear chain of regular
      octahedra sharing one corner for which the
      octahedron rotation angle is $\omega_0 = \pi/6$.
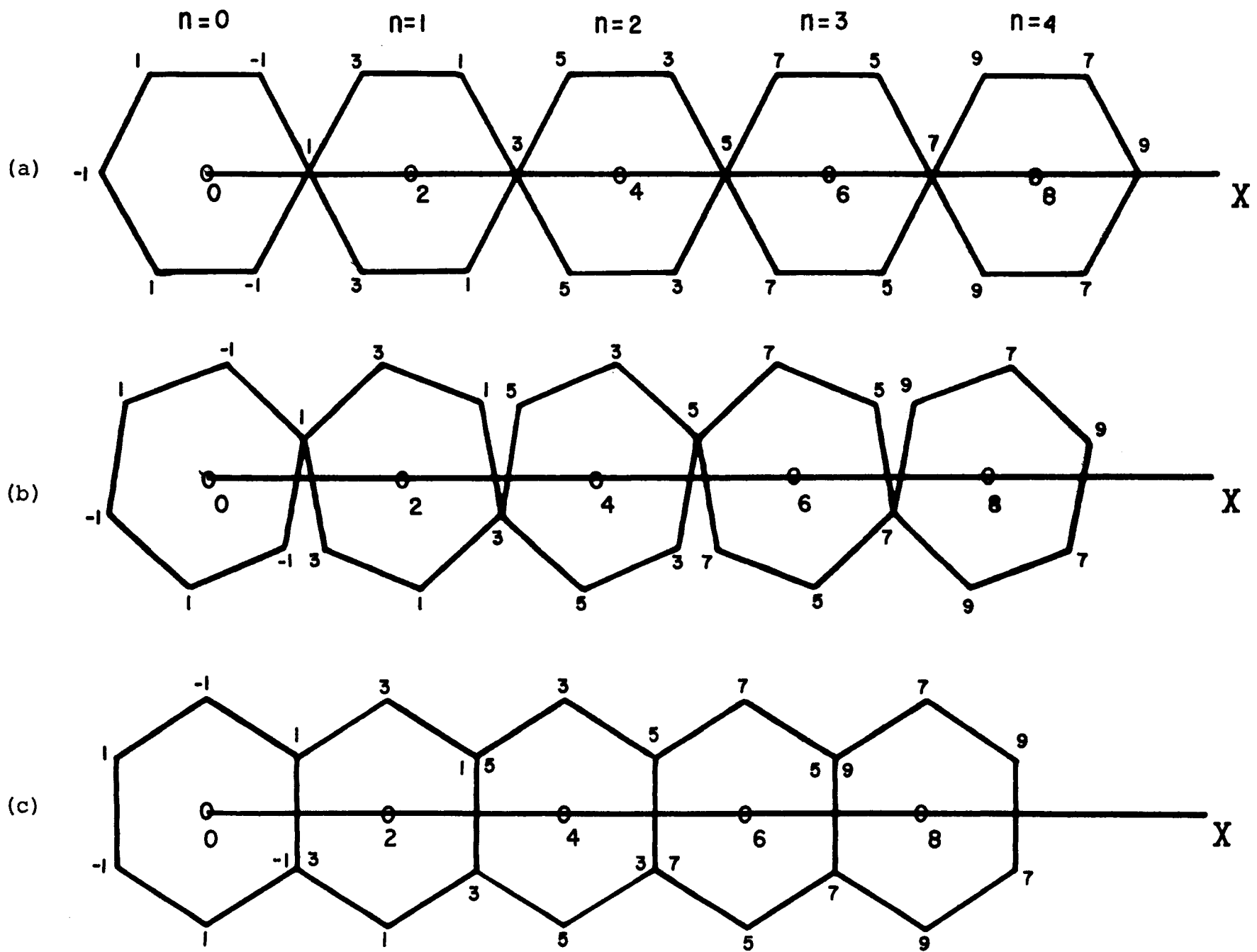
Figure 2

Thus, by continuity from the configuration in Fig. 2a, the configuration in Fig. 2c is reached, for which the octahedron rotation angle is $\omega_o = \frac{\pi}{6}$.

In the following it will be shown how this continuous transformation ($|\omega| < \frac{\pi}{6}$) occurs in a three-dimensional octahedral framework.

Due to the octahedral symmetry, a three-fold rotation around $\underline{\Delta}_o$ of an octahedron $\underline{n}$ is equivalent to a translation of all the original octahedron coordinates.

As is shown in Fig. 3, the three octahedra ($n = 1$), equivalent by three-fold rotation, are related by the translation vectors:

$$\vec{a}_i = [3]^i \cdot \begin{bmatrix} -2 \cos \omega \\ +2 \cos \omega \\ 0 \end{bmatrix} \qquad (i = 1,2,3) \tag{6}$$

where the matrix [3] represents the three-fold rotation around Δ_o:

$$[3] = [6]^2 = \begin{bmatrix} 0 & \bar{1} & 0 \\ 1 & \bar{1} & 0 \\ 0 & 0 & 1 \end{bmatrix}$$

The three equivalent octahedra, $\underline{n}$, are related by the three vectors $n\vec{a}_i$ ($i = 1,2,3$).

Figure 3. Three-fold rotation around OZ of a linear chain of regular octahedra n = 1, 2, 3..., onto a plane perpendicular to OZ.
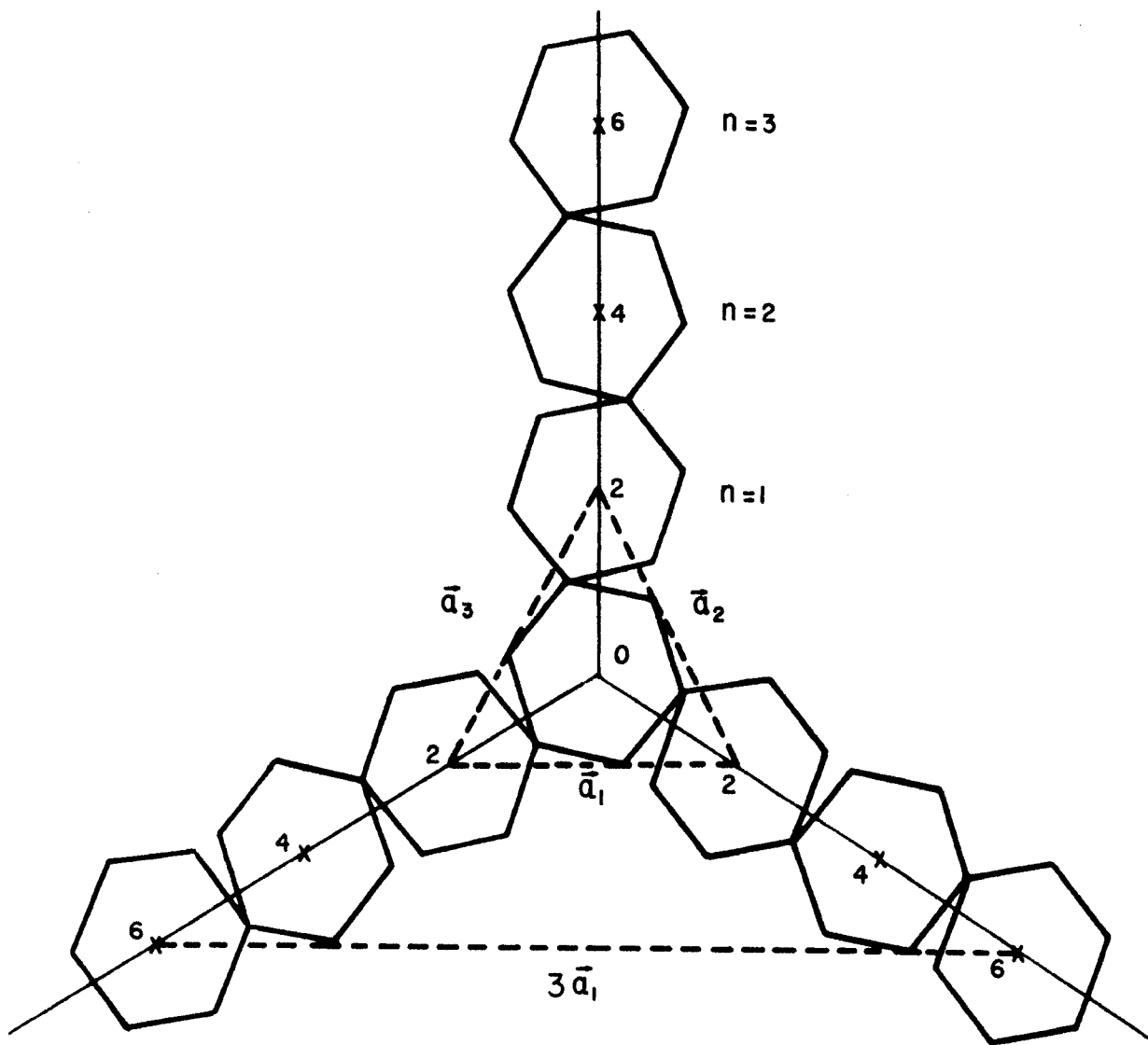
Therefore, a three-fold rotation of linear chain around each Δ_n generates a three-dimensional framework of regular octahedra sharing corners (Fig. 4). The octahedra corners lie on parallel planes intersecting $\vec{O}_z$ in $z = 2n + 1$ and are related in these planes by the vectors $\vec{a}_i$. Thus, a two dimensional lattice is defined in the (x,y) plane by two vectors $\vec{a}_1$, $\vec{a}_2$ with the periodicity along these two directions:

$$a = |\vec{a}_i| = 2 \underline{e} \cdot \cos \omega \tag{7}$$

To determine the periodicity along the $\vec{O}_z$ direction, reference is made to a new set of hexagonal axes $(\vec{a}_1, \vec{a}_2, \vec{k})$.

The new parameters of the octahedra centers are given by:

$$\vec{OO}_n = n \cdot \begin{bmatrix} 1/3 \\ 2/3 \\ 2 \end{bmatrix} \qquad \text{with } (n = 0,1,2\ldots)$$

where the rotation angle ω_n is defined as previously:

$$\omega_n = (-1)^n \omega_o$$

Thus, in the $\vec{O}_z$ direction, the octahedron $n = 6$ is the next equivalent one to be rotated by the same angle as the
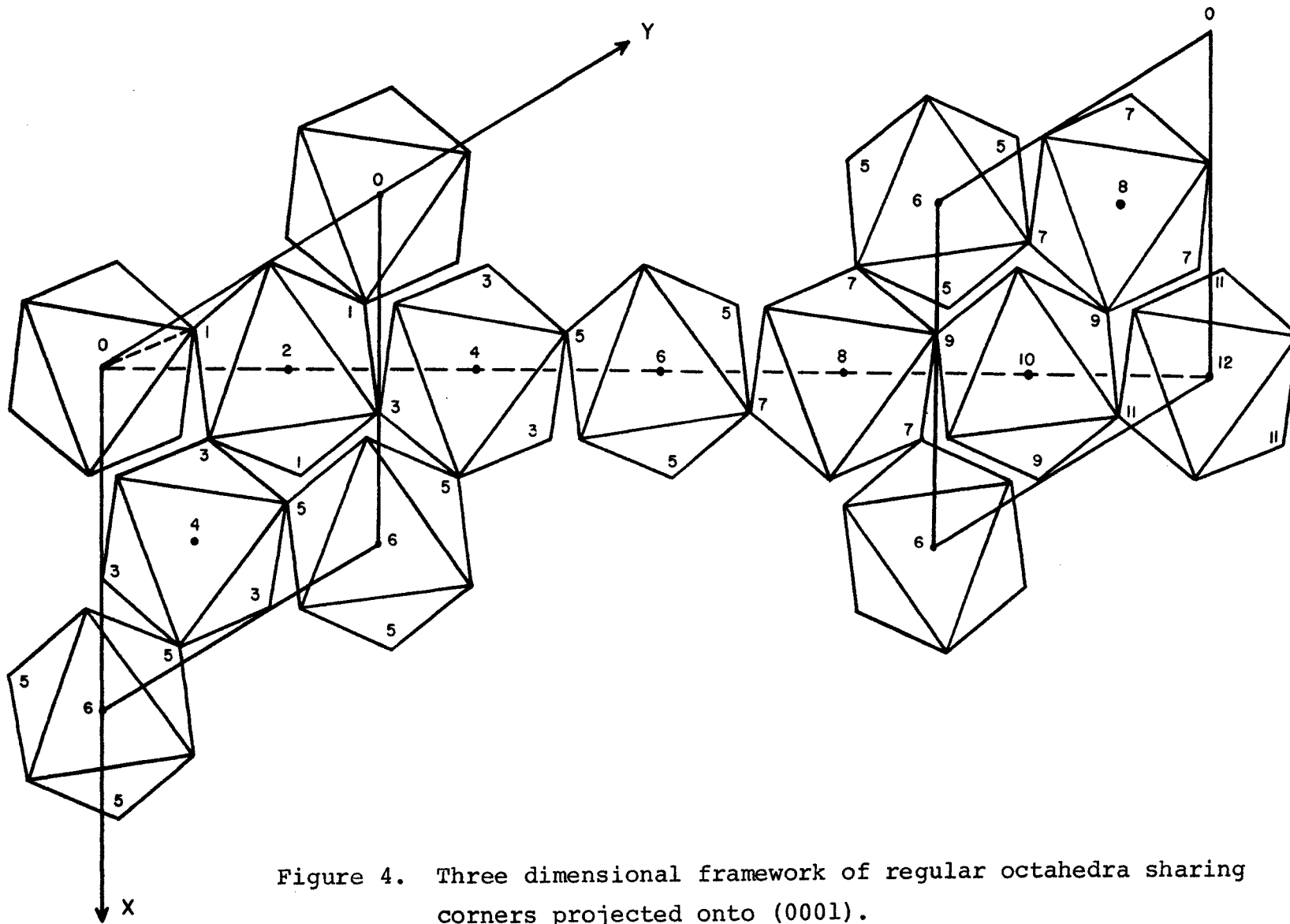
Figure 4. Three dimensional framework of regular octahedra sharing corners projected onto (0001).

octahedron n = o. A hexagonal cell is then defined by the
vectors $(\vec{a}_1, \vec{a}_2)$ in the (x,y) plane and by $\vec{c} = 12 \vec{k}$ along
$\vec{O}_z$. In this cell, the coordinates of the octahedron
centers are:

$$\vec{OO}_n = n \cdot \begin{bmatrix} 1/3 \\ 2/3 \\ 1/6 \end{bmatrix}$$

Consequently, within the hexagonal cell, the octahedra
n, n + 2, n + 4...., are rotated in the same way with the
equivalent coordinates of their corners related by the
translation vectors

$$\vec{R}_1 = (1/3, 2/3, 2/3) \text{ and } \vec{R}_2 = (2/3, 1/3, 1/3).$$

These vectors represent the rhombohedral lattice
operator $\vec{R}_+ = (2/3, 1/3, 1/3)_+$.

Therefore, the true symmetry is rhombohedral and the
volume of the unit rhombohedral cell is three times smaller
than the volume of the hexagonal cell.

The structure is more easily visualized by referring
to the hexagonal cell. Fig. 4 shows this framework in
projection onto (0001) with a height expressed in 1/12
units.

The octahedron n, with its center lying on the plane
$z = n/12$, shares its three upper corners in $z = \dfrac{2n + 1}{12}$,

with three different octahedra centered in $z = \dfrac{2n + 2}{12}$.

Similarly, its three lower corners are shared in $z = \dfrac{2n - 1}{12}$ with three different octahedra centered in $z = \dfrac{2n - 2}{12}$. The corners of these regular octahedra form an array of six equidistant layers in this hexagonal cell, parallel to (0001).

The center and the three-fold axes of each octahedron both coincide with the centers of symmetry and the three-fold axes of the entire lattice.

2. <u>Theoretical relationships</u>. The octahedron, $n = o$, shares the corner $\underline{P}_o$ with the octahedron, $n = 1$, centered at O_1. In the following, γ and γ' correspond to the angles of $O\underline{P}_o$ and OO_1, respectively, with the (xy) plane.

If the angle $\widehat{OP_oO_1} = \phi$, we have the relationships:

$$\sin \phi/2 = \frac{\cos \omega \cos \gamma}{\cos \gamma'} \qquad (8)$$

with

$$\tan \gamma = \frac{|\vec{k}|}{|\vec{i}|} = \frac{1}{\sqrt{2}}$$

and

$$\tan \gamma' = \frac{|\vec{k}|}{|\vec{i}| \cos \omega}$$

O_1', P_1, P_3, P_5 correspond to the projection of O_1 and the 3 upper corners P_1, P_3, P_5 of the octahedron,

n = 1, onto the xy plane as shown in Fig. 5.

From the geometry,

$$\omega = \overparen{O\ O_1 P_o} \qquad \overparen{O_1\ O\ P_1} = \pi/6 \text{ and } \vec{op}_1 = \begin{bmatrix} x \\ 0 \\ 0 \end{bmatrix}$$

Therefore, the three upper corner coordinates of the octahedron n = 1 can be expressed in the hexagonal cell by:

$$[3]^i \cdot \begin{bmatrix} x \\ 0 \\ 1/4 \end{bmatrix} \qquad (i = 1,2,3)$$

with

$$x = \frac{2\ \ell}{|a_i|} \cos\left(\omega + \frac{\pi}{6}\right) = \frac{\sqrt{3}\ \cos\ \omega\ -\ \sin\ \omega}{2\sqrt{3}\ \cos\ \omega}$$

$$(9)$$

By a translation of $-\vec{c}/2$ from this octahedron, one arrives at the octahedron, n = -2, rotated in the opposite way with its coordinates of the three upper corners as:

$$-[3]^i \cdot \begin{bmatrix} x \\ 0 \\ 1/4 \end{bmatrix} \qquad (i = 1,2,3)$$

With the translation vectors $\vec{R}_+$, the positions of all the octahedral corners can be generated in the hexagonal cell. These positions, entirely defined in this cell by a single parameter, x , are given by:
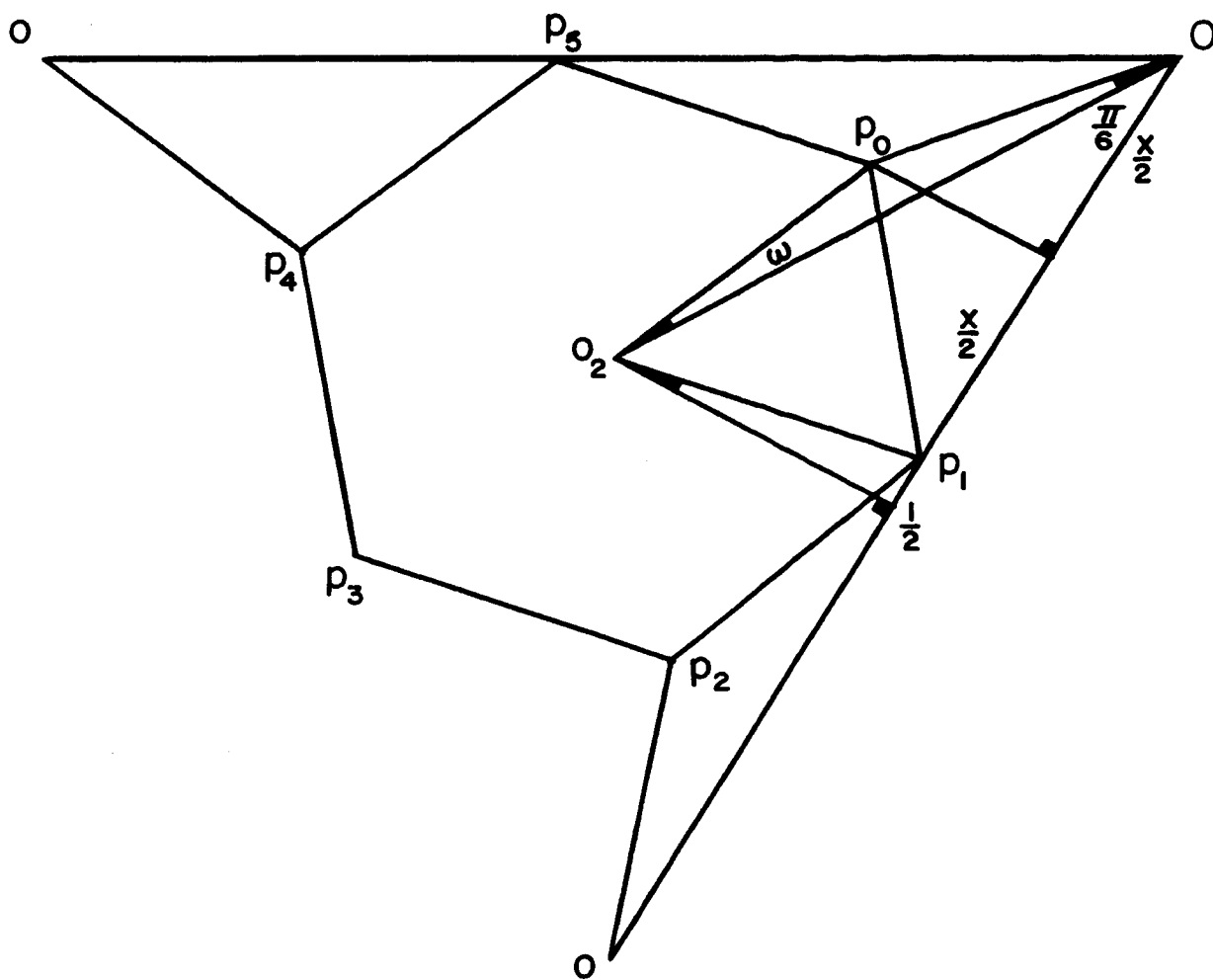
Figure 5. Projection of the octahedron n = 2 onto (0001).

$$\pm[3]^i \cdot \begin{bmatrix} x \\ 0 \\ 1/4 \end{bmatrix} + \vec{R}_+ \quad (i = 1,2,3)$$

Thus, in this hexagonal unit cell we have 18 equivalent positions as follows:

$$x, \ 0, \ 1/4; \ 0, \ x, \ 1/4; \ \bar{x}, \ \bar{x}, \ 1/4$$

$$\bar{x}, \ 0, \ 3/4; \ 0, \ \bar{x}, \ 3/4; \ x, \ x, \ 3/4$$

with the translation vector $\vec{R}_+$ = (0,0,0; 1/3, 2/3, 2/3 ; 2/3, 1/3, 1/3)+ . These coordinates are the equivalent positions 18e in the space group $R\bar{3}c$, (origin at $\bar{3}$).

The axial ratio c/a of the hexagonal cell parameter is calculated from equations (1), (4):

$$c/a = \frac{\sqrt{6}}{\cos \omega} \tag{10}$$

From equations (5), (6), x and ϕ can be expressed as functions of c/a

$$x = 1/2 - 1/6 \sqrt{\frac{[c/a]^2 - 6}{2}} \tag{11}$$

$$\phi = 2 \ \text{Arcsin} \sqrt{1/3 + \frac{4}{(c/a)^2}} \tag{12}$$

The axial ratio c/a of the hexagonal cell is related to the angle α of the corresponding rhombohedral cell by:

$$(c/a)^2 = \frac{9}{4 \sin^2 \frac{\alpha}{2}} - 3 \qquad (13)$$

Then,

$$\alpha = \text{Arcos} \left[\frac{1 + 4 \ (1-2x)^2}{2 + 4 \ (1-2x)^2}\right] \qquad (14)$$

The angular relationship between α and ϕ is independent of the cell parameters:

$$\alpha = \text{Arcos} \left[\frac{5 + \cos \phi}{6 - 2 \cos \phi}\right] \qquad (15)$$

If $\omega = 0$, then c/a $= \sqrt{6}$; $\alpha = \frac{\pi}{3}$; $x = 1/2$; $\phi = \pi$, characteristic of the octahedral framework in the ideal perovskite configuration.

If $\omega = \frac{\pi}{3}$, then c/a $= \sqrt{8}$; $\alpha_H = 2 \text{ Arcsin } \sqrt{9/44} = 53°50'$

$$x = \frac{1}{3} \text{ and } \phi = 132° = 2 \text{ Arcsin } \sqrt{5/6}$$

This configuration is the hexagonal close-packed array.

From this geometrical approach, it has been shown that it is topologically possible by rotating the regular octahedra around their three-fold axes to transfrom continuously from a hexagonal close-packed configuration to

an ideal octahedral framework of the perovskite-like configuration.

The proposed model ($0 < |\omega| < \frac{\pi}{6}$) belongs to R$\bar{3}$c and can be viewed as being generated by an array of linear chains. Such a framework can be considered as an intermediate between the hexagonal close-packed and the cubic close-packed configuration with the corner sites of each face centered cube left vacant. In the following, this vacancy which is surrounded by 12 corner sites of the octahedra is called $\boxed{A}$ (site a). The volume of this vacancy decreases when ω increases.

B   (site b) corresponds to the center of each octahedron. In the hexagonal cell the positions in the sites $\underline{a}$ and $\underline{b}$ are give by:

$$(0, 0, 1/4; \ 0, 0, 3/4) + \vec{R}_+ \quad \text{positions 6a}$$

$$(0, 0, 0; \quad 0, 0, 1/2) + \vec{R}_+ \quad \text{positions 6b}$$

In reality, in a wide range of compounds based on such octahedral framework of anions, the sites $\underline{a}$ or $\underline{b}$ are occupied by atoms. As a result, each octahedron is distorted but in most cases, the spread of the octahedral edge distance around the mean value is very small. Therefore, these octahedra can be regarded as regular to a first approximation, and the resulting anionic framework is derived from this proposed model. Inasmuch as this

approximation of "regular octahedron" is valid, the pre-
ceding relationships must also be valid. In order to
verify these relationships, a group of different rhombo-
hedral compounds containing this octahedral framework will
be examined.

C. Correlations in a Series of Ferroelectric Compounds
in Terms of Trigonal Rotation of BO_6 Octahedra

1. Description of the structures. The crystal
structures of ferroelectric $BiFeO_3$ and $PbZr_{0.9}Ti_{0.1}O_3$ have
been reported recently.[21,22] In these isomorphous perov-
skite-type compounds, the rhombohedral unit cell contains
two formula units. The parameter $\underline{a}_R$ is the face diagonal
of the unimolecular perovskite-like subcell, Fig. 6. The
relations between the face centered pseudocubic cell and
the primitive rhombohedral cell are:

$$\underline{a}_R = 1/2 \ \underline{a}_f \ \sqrt{2(1 + \cos \alpha_f)}$$

$$\cos \alpha_R = 1/2 \ \frac{3 \cos \alpha_f + 1}{\cos \alpha_f + 1} \quad ,$$

where $\underline{a}_f$ and α_f denote the pseudocubic parameters and the
rhombohedral angle α_R is nearly $60°$.

Fig. 7 shows the shift of the atoms from the ideal
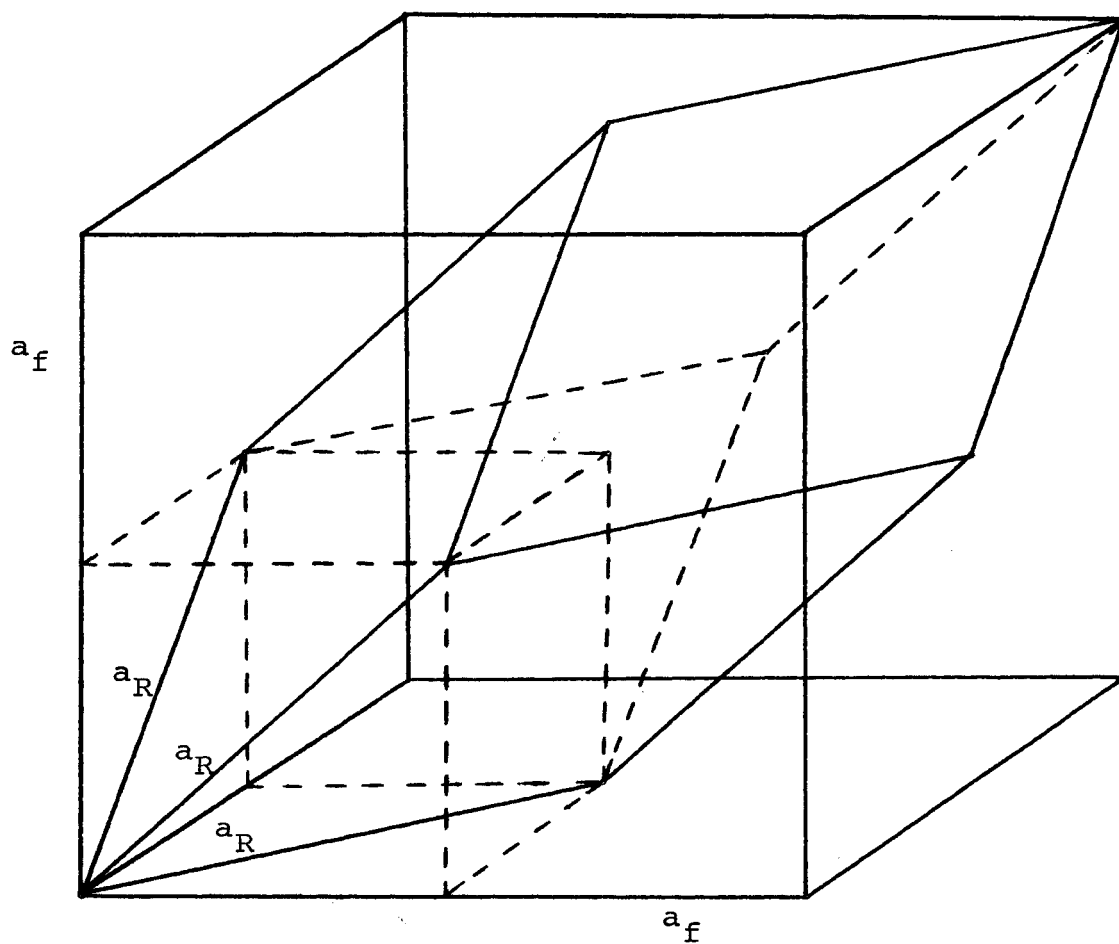perovskite positions. The two cations are shifted in the

Figure 6. Primitive rhombohedral cell derived from multiple pseudocubic cell.
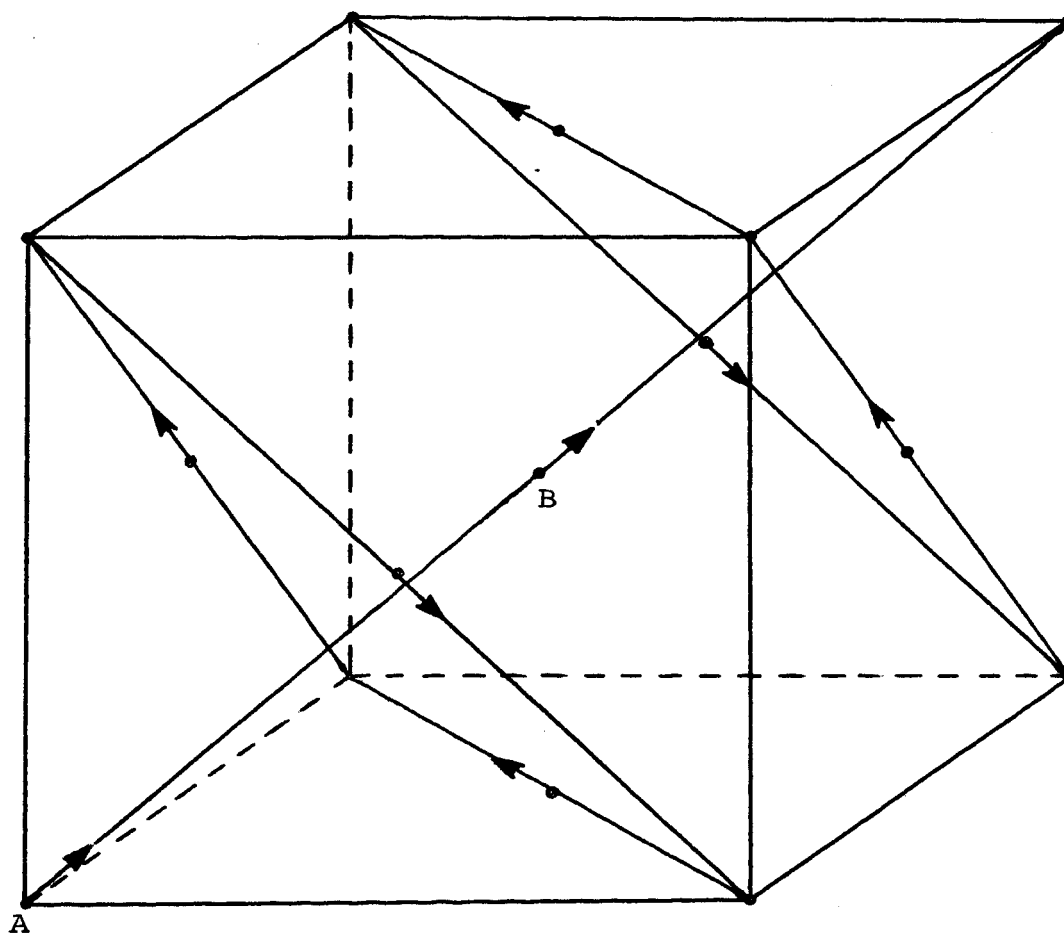
Figure 7. Atom shifts in the pseudocubic perovskite cell.

same direction along [111]. The oxygens rotate around the trigonal axis in the same type of oxygen shift as observed for $LaAlO_3$. The resulting space group is R3c.

For the following discussion, it is convenient to transform the rhombohedral cell into the corresponding hexagonal cell containing six formula units. The unit vectors of the true cell can be related to the perovskite cell by the matrix:

$$\begin{bmatrix} 0 & 1 & 1 \\ 1 & 0 & 1 \\ 1 & 1 & 0 \end{bmatrix}$$

and to the hexagonal cell by the matrix:

$$\begin{bmatrix} \frac{2}{3} & \frac{1}{3} & \frac{1}{3} \\ -\frac{1}{3} & \frac{1}{3} & \frac{1}{3} \\ -\frac{1}{3} & \frac{2}{3} & \frac{1}{3} \end{bmatrix}$$

The oxygen atoms are arranged in six equidistant planar layers normal to and intersecting the $\underline{c}$ axis at z = 1/12 $(2\underline{n} + 1)$, where $\underline{n}$ is integral.

The atomic parameters of the ideal perovskite-like framework are: Fig. 8a,

$$\begin{array}{llll} A & 0, & 0, & 0 \\ B & 0, & 0, & 1/4 \\ O & 1/6, & 1/3, & 1/12 \end{array}$$
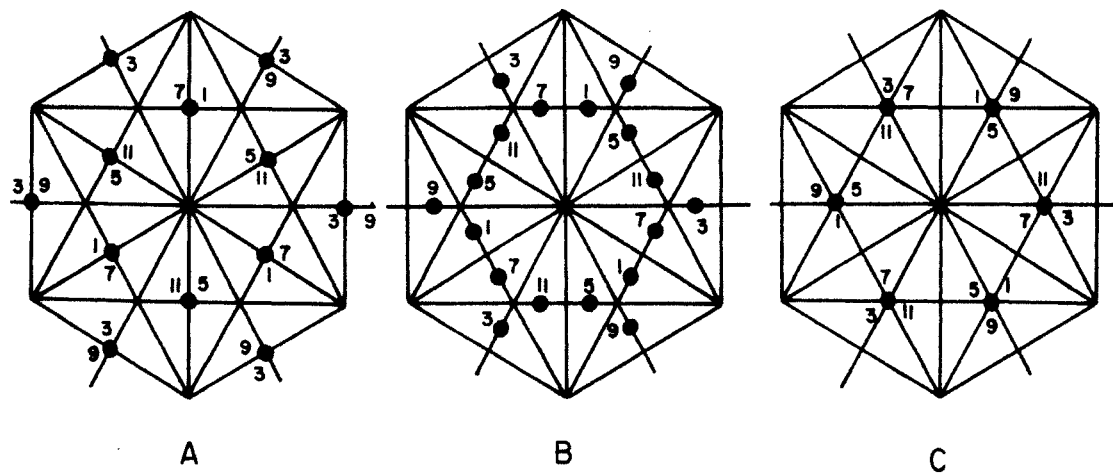
Figure 8. Projection of oxygen onto the (0001) plane.

    A.   Oxygen framework in ideal perovskite.

    B.   Intermediate framework.

    C.   Ideal hexagonal close-packed oxygen framework.

We may write the parameters of both $BiFeO_3$ and $PbZr_{0.9}Ti_{0.1}O_3$ as follows:

A   0, 0, $\underline{w}$

B   0, 0, 1/4 + $\underline{w}'$

O   1/6 - $\underline{u}$, 1/3 + $\underline{v}$, 1/12

where $\underline{w}$, $\underline{w}'$, $\underline{u}$, and $\underline{v}$ express the atomic shift from the ideal positions.

Fig. 8b describes the oxygen shifts from their ideal perovskite positions for different values of $\underline{n}$. The heavy atom B lies at the center of an oxygen octahedron oriented with two opposite faces perpendicular to the $\underline{c}$ axis.

Table I gives the values of the lengths of different oxygen octahedron edges. The spread of the oxygen distances around the average value is very small. Therefore, the oxygen positions can be considered as resulting from a rotation around the $\underline{c}$ axis from the ideal position of a rigid octahedron. The rotation of the octahedron is evaluated by an angle ω given by the relation:

$$\cos \omega = \frac{\vec{OM} \cdot \vec{OP}}{|\underline{OM}| \; |OP|}$$

where $\underline{O}$ is the center of the octahedron and $\underline{M}$ is the projection onto the (0001) plane of the octahedral corners tilted from the ideal perovskite position $\underline{P}$, Fig. 9.
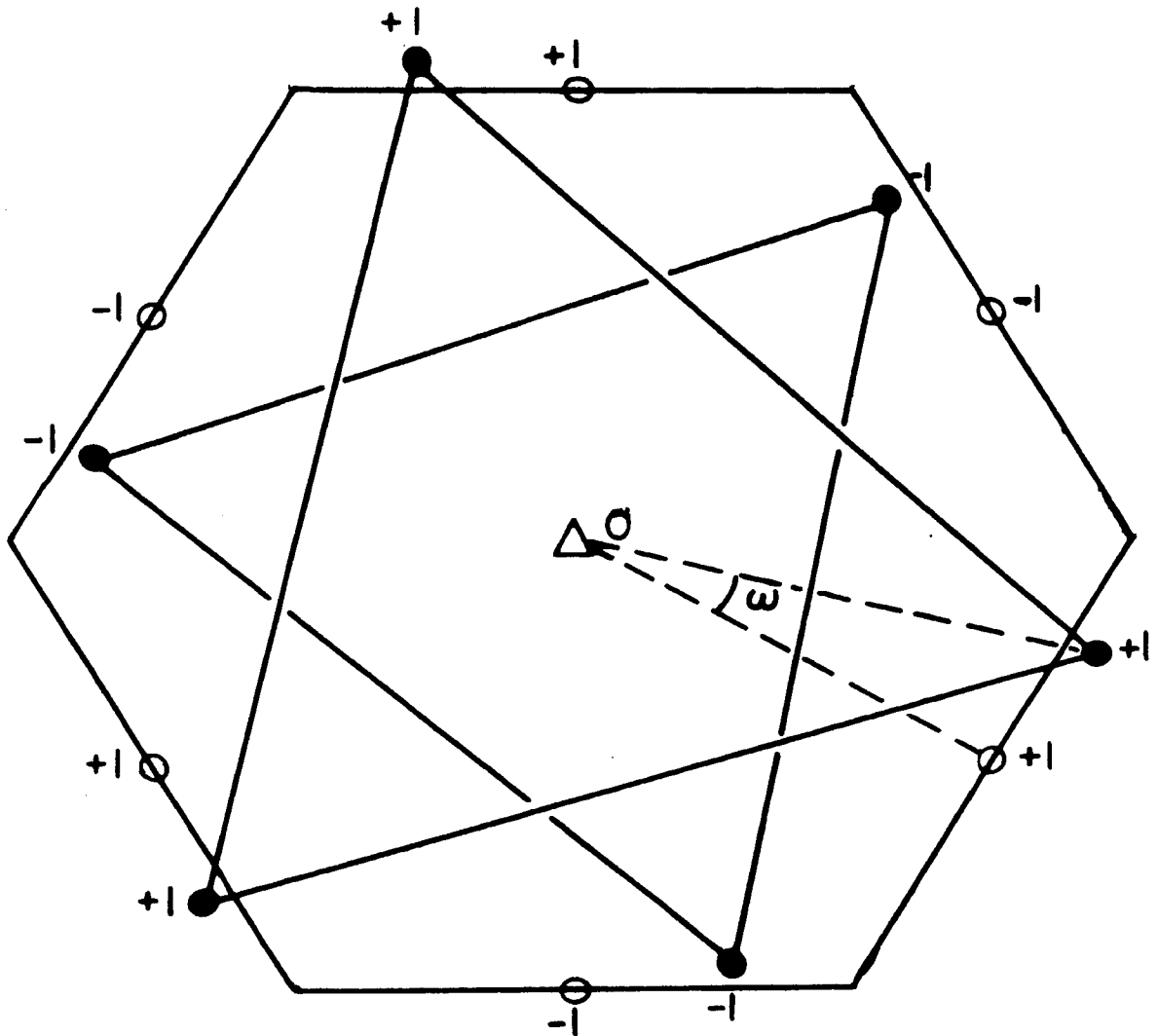
Figure 9

ROTATION, ᘯ , AND SLIGHT DISTORTION OF ONE OXYGEN
OCTAHEDRON CENTERED AT ORIGIN.

o PEROVSKITIC POSITION   ● SHIFTED POSITION
   OF OXYGEN   OF OXYGEN

TABLE I

OXYGEN OCTAHEDRA EDGES IN $\overset{\circ}{A}$

| $PbZr_{0.9}Ti_{0.1}O_3$	$BiFeO_3$	$LiNbO_3$
3.04	2.89	2.879
2.85	2.76	2.719
2.93	2.84	2.801
2.94	2.87	2.840

According to Megaw[31] it is topologically possible to trans-
form an octahedral framework continuously from the ideal
perovskite configuration to the hexagonal close-packed
configuration. This transformation may be realized by
rotating the rigid BO_6 octahedron around the $\underline{c}$ axis as
shown in Fig. 10. When ω attains the value of 30 degrees,
the oxygen framework is then hexagonal close-packed, Fig.
8c, the oxygen atom coordinates being 0, 1/3, 1/12. In a
note, Megaw[42] considered oxygen octahedra in $LiNbO_3$ as
rotated around their triad axis by an angle of 6.5° from
the ideal hexagonal close-packed position and pointed out
that with increasing temperature this structure could be
looked upon as a highly distorted perovskite-type.

Thus, we can consider the oxygen array in $PbZr_{0.9}Ti_{0.1}O_3$
and $BiFeO_3$ as being in the early stage of a continuous
transformation which is fully developed in $LiNbO_3$ and the
isomorphous $LiTaO_3$.

2. Theoretical Relationships. In this isomorphous
series, the different stages of the rotation of oxygen
octahedra give rise to a variation of both the hexagonal
cell parameter $\underline{a}$ and the rhombohedral angle α. A theo-
retical relationship will now be derived between the
angles ω and α.

For any value of the tilt angle ω, the rigid octa-
hedron is a regular hexagon in projection with a constant
edge length, $\underline{\ell}$. The hexagonal cell parameter $\underline{a}$ depends
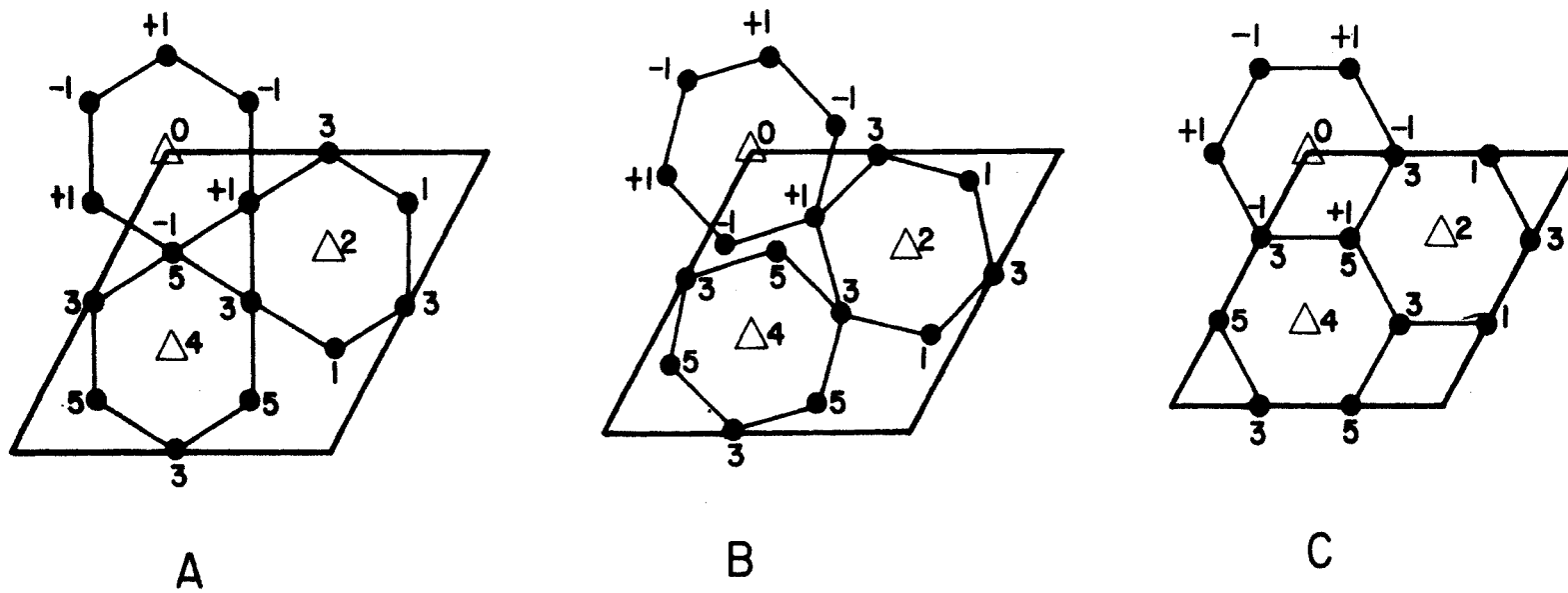
PROJECTIONS OF OXYGEN ATOMS ONTO THE (0001) PLANE FOR ONE HALF OF THE CELL:

A. PEROVSKITIC OXYGEN FRAMEWORK.   B. INTERMEDIATE OXYGEN FRAMEWORK.

C. IDEAL HEXAGONAL CLOSE-PACKED OXYGEN FRAMEWORK.

Figure 10.   Octahedral framework rotation.

only on the rotation of the octahedra, Fig. 10.
Thus, for the ideal perovskite configuration:

$$\underline{a} = 2\underline{\ell}\sqrt{3} = \underline{a}_p$$

For the intermediate configurations corresponding to
oxygen shifts from this idealized system, Figs. 8b and
10b :

$$\underline{a}_{(\omega)} = 2\underline{\ell} \cos (\frac{\pi}{6} - \omega) + 2\underline{\ell} \cos (\frac{\pi}{6} + \omega)$$

$$\underline{a}_{(\omega)} = 2\underline{\ell}\sqrt{3} \cos \omega = \underline{a}_p \cos \omega \qquad (16)$$

For the hexagonal close-packed configuration:

$$\underline{a}_H = \underline{a}_p \sqrt{3/2}$$

During the continuous transformation from the octa-
hedral framework in the ideal perovskite ($\omega = 0$) to the
hexagonal close-packed framework ($\omega = \frac{\pi}{6}$), the hexagonal
cell parameter $\underline{a}$ decreases while $\underline{c}$ remains constant. The
general relation between the axial ratio c/a of the
hexagonal cell and the angle α of the corresponding
rhombohedral cell is:

$$(c/a)^2 = \frac{9}{4 \sin^2 (\frac{\alpha}{2})} - 3$$

or

$$\cos \alpha = 1 - \frac{9}{6 + 2(c/a)^2} \qquad (17)$$

Therefore, for the oxygen configuration in the ideal perovskite,

$$\alpha_p = \frac{\pi}{6} \quad \text{and} \quad c/a_p = \sqrt{6} \quad ,$$

whereas for the hexagonal close-packed configuration,

$$\alpha_H = 53°50' \text{ and } c/a_H = \sqrt{8} \quad .$$

From equation (16) one can calculate the ratio

$$c/a_\omega = \frac{\sqrt{6}}{\cos \omega} \quad ,$$

which when combined with equation (17) gives α as a function of ω:

$$\alpha = \text{Arc } \cos \frac{4 - \cos^2 \omega}{4 + 2 \cos^2 \omega} \qquad (18)$$

This angular relationship is independent of the cell parameters and therefore can be applied to any rhombohedral compounds with this type of deformation.

The ratio,

$$\kappa = \frac{\Delta\alpha}{\Delta\alpha_M} = \frac{\alpha_p - \alpha}{\alpha_p - \alpha_H}$$

where $\Delta\alpha_M$ represents the maximum change in rhombohedral angle, increase from 0 for the octahedral framework of the ideal perovskite ($\omega = 0$), to 1 when this framework becomes hexagonal close-packed ($\omega = \omega_M = \frac{\pi}{6}$). κ can be expressed in reduced coordinates by the following equation:

$$\kappa = \frac{1}{\alpha_p - \alpha_H} \left[\frac{\pi}{3} - \text{Arcos} \left\{ \frac{7 - \cos\left(\frac{\pi}{3} \cdot \frac{\omega}{\omega_M}\right)}{10 + 2\cos\left(\frac{\pi}{3} \cdot \frac{\omega}{\omega_M}\right)} \right\} \right]$$

$$(19)$$

$\kappa \rightarrow 0$ and $\frac{\omega}{\omega_M} \rightarrow 0$ as the oxygen array approaches that of the ideal perovskite-like configuration. Conversely, as the oxygen array approaches that found in the hexagonal close-packed arrangement, $\kappa \rightarrow 1$ and $\frac{\omega}{\omega_M} \rightarrow 1$.

Table II lists the different values of ω and $\Delta\alpha$ for the compounds $LaAlO_3$, $PbZr_{0.9}Ti_{0.1}O_3$, $BiFeO_3$, $LiTaO_3$, and $LiNbO_3$. The theoretical curve as derived from relation (19) is plotted in Fig. 11.

TABLE   II

OCTAHEDRAL TILT ANGLE ω AND

CORRESPONDING RHOMBOHEDRAL ANGLE DIFFERENCE $\Delta\alpha$

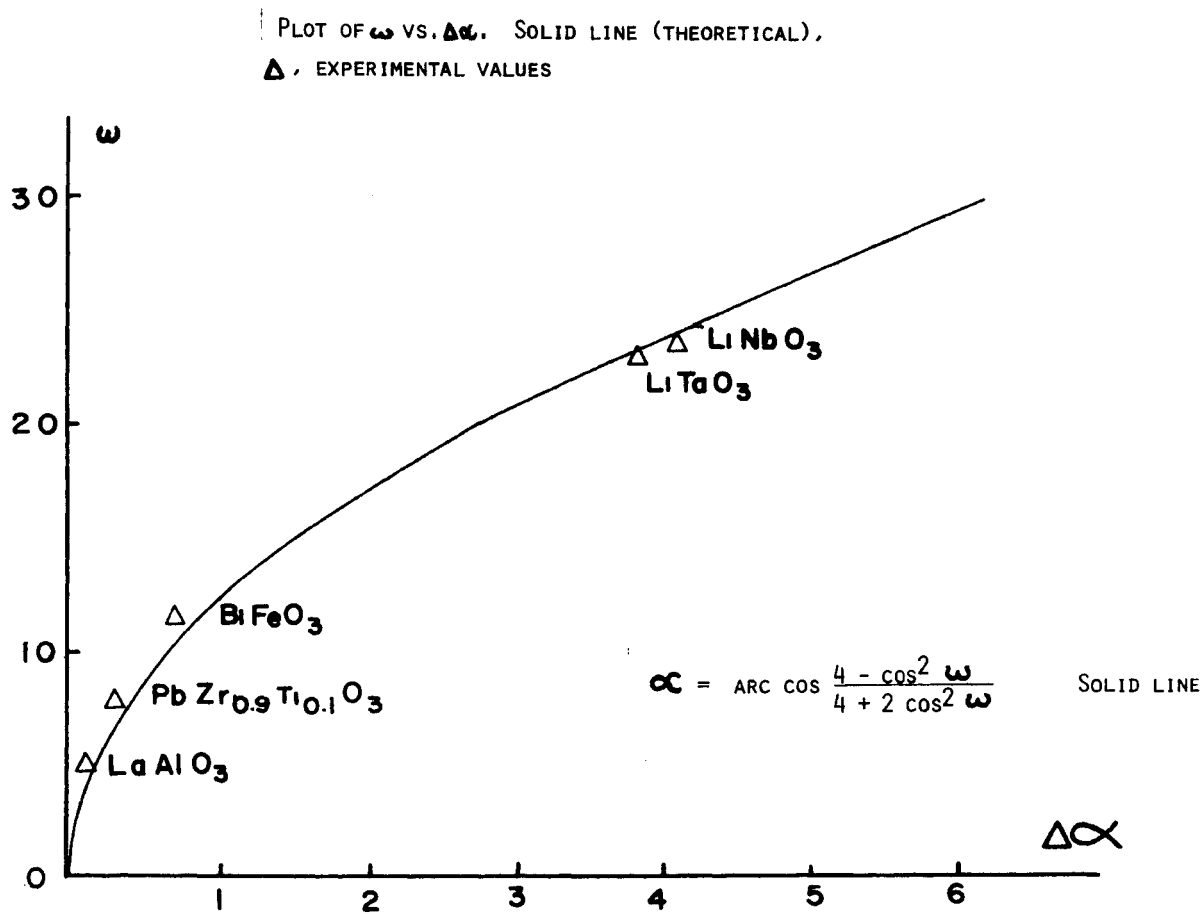|	ω	$\Delta\alpha = \alpha_p - \alpha$
$LaAlO_3$	5°40'	6'
$Pb(Zr_{0.9}Ti_{0.1})O_3$	8°	18'
$BiFeO_3$	11°40'	42'
$LiTaO_3$	23°	3°50'
$LiNbO_3$	23°30'	4°08'

Figure 11

THE ROTATION ω OF AN OCTAHEDRAL FRAMEWORK AROUND A TRIGONAL AXIS AS IN $LaAlO_3$, AND THE CORRESPONDING RHOMBOHEDRAL CELL ANGLE α CAN BE RELATED. A THEORETICAL RELATIONSHIP IS REPORTED BETWEEN α AND ω AND VERIFIED FOR A PEROVSKITE-TYPE SERIES IN THE $R3c$ SPACE GROUP.

The experimental values reported from the preceding series are in good agreement with this relationship. The spread of the observed values around the theoretical curve can be attributed to experimental error and also to the fact that the oxygen octahedra are not regular but slightly distorted.

D. Theoretical Relationships Applied to Some Perovskite-Type Series and Related Trifluoride Compounds

1. BF_3 series. A series of trifluoride compounds is first considered. The octahedral framework is composed of fluoride atoms. These compounds can be expressed in terms of vacancy $\boxed{A}$ by: $\boxed{A}$ BF_3, where B is a transition metal in the site b. These compounds have been classified into three groups.[32]

a.   The group MoF_3 where F corresponds to the configuration $\omega = 0$. This group forms the series MoF_3, TaF_3, NbF_3, isostructural with ReO_3. This structure may be described as cubic close-packing of fluorine atoms in which the octahedral interstices are occupied by metal atoms forming a simple cubic superlattice, and in which one quarter of the fluorine atom sites, those not adjacent to metal atoms, remain vacant.

b.   The group PdF_3 with Pd in site b and F in the octahedral configuration corresponding to $\omega = \frac{\pi}{6}$. PdF_3, RhF_3, and IrF_3 are isostructural with the fluorine array

in a hexagonal close-packed configuration.

    c.   The VF_3 group where the fluoride framework is intermediate between the arrangements of type (a) and (b). This group forms the isostructural series VF_3, FeF_3, CoF_3, RuF_3, TiF_3.

The rhombohedral unit cell is bimolecular. These structures consist of alternately and regularly spaced planes of metals and planes of fluorine atoms perpendicular to the trigonal (hexagonal c) axis. Each octahedron is not perfectly regular but is expanded by the presence of the cation by about 3% in length along its trigonal axis. Accordingly, the spread of the F-F distance on the average is very small (less than 2%). Table III gives the rhombohedral parameters α and c/a for all these compounds and the corresponding ϕ bond angle (ϕ = M-F-M).

In Fig. 12 the solid line represents the theoretical plot c/a versus ϕ as calculated from equation (12).

In Fig. 13 the solid line represents the theoretical plot of α versus x from equation (14).

Equations (12) and (14) are in excellent agreement with the experimental values Δ shown in Figs. 12 and 13.

    2. Perovskite-type series. A series of perovskite-type compounds ABO_3 is also examined. $LaCoO_3$[43] is iso-morphous with $LaAlO_3$.[20] These structures are in the $R\bar{3}c$ space group with the oxygen positions in 18e; La in site $\underline{a}$. (Parameters are given in Table III). In these

TABLE III

CRYSTALLOGRAPHIC PARAMETERS

Compounds	c/a	$\phi = M-X-M$ [*]	α_R	x_h [**]
$LiNbO_3$	2.693	142.00	55.89	0.382
$LiTaO_3$	2.674	143.04	56.17	0.383
$BiFeO_3$	2.493	160.04	59.30	0.445
PZT	2.465	166.33	59.70	0.463
$LaCoO_3$	2.492	163.20	59.23	0.447
$LaAlO_3$	2.462	172.11	59.90	0.475
VF_3	2.592	147.00	57.52	0.395
TiF_3	2.502	158.80	59.07	0.433
FeF_3	2.564	153.00	57.99	0.419
CoF_3	2.625	149.00	56.97	0.400
RuF_3	2.769	136.00	54.67	0.350
RhF_3	2.786	132.00	54.42	0.333
PdF_3	2.818	132.00	53.92	0.333
IrF_3	2.797	132.00	54.13	0.333
$(Mo, Ta, Nb)F_3$	2.449	180.00	60.00	0.500

[*] ϕ is the bond angle MOM or MFM where M is a metal atom occupying the site 6b (R3c or R$\bar{3}$c).

[**] x_h is the octahedral framework parameter in the hexagonal cell with the axial ratio c/a.

Figure 12. Hexagonal axial ratio dependence of the bond angle ϕ ($\stackrel{\frown}{M \times M} = \phi$).
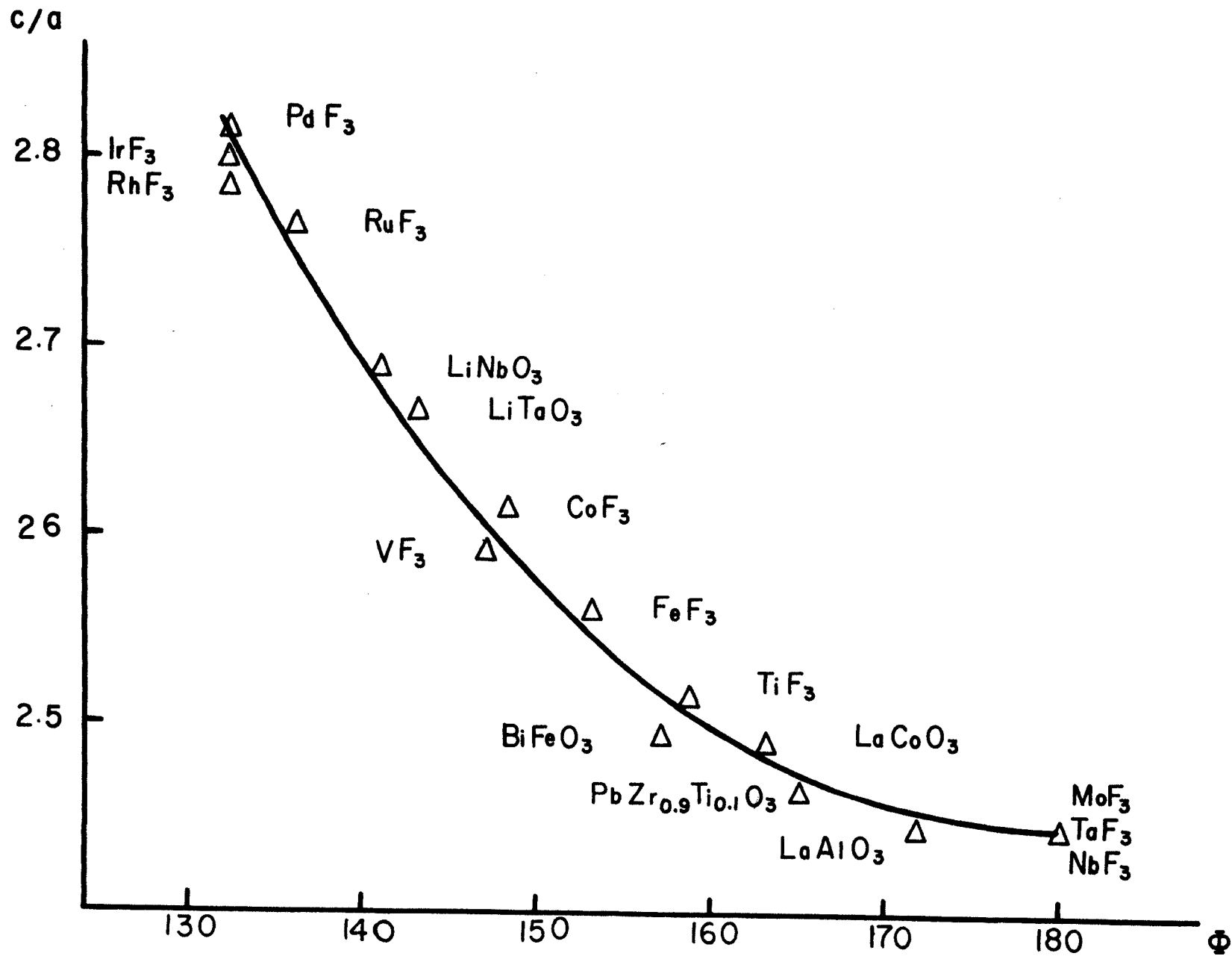
Figure 12

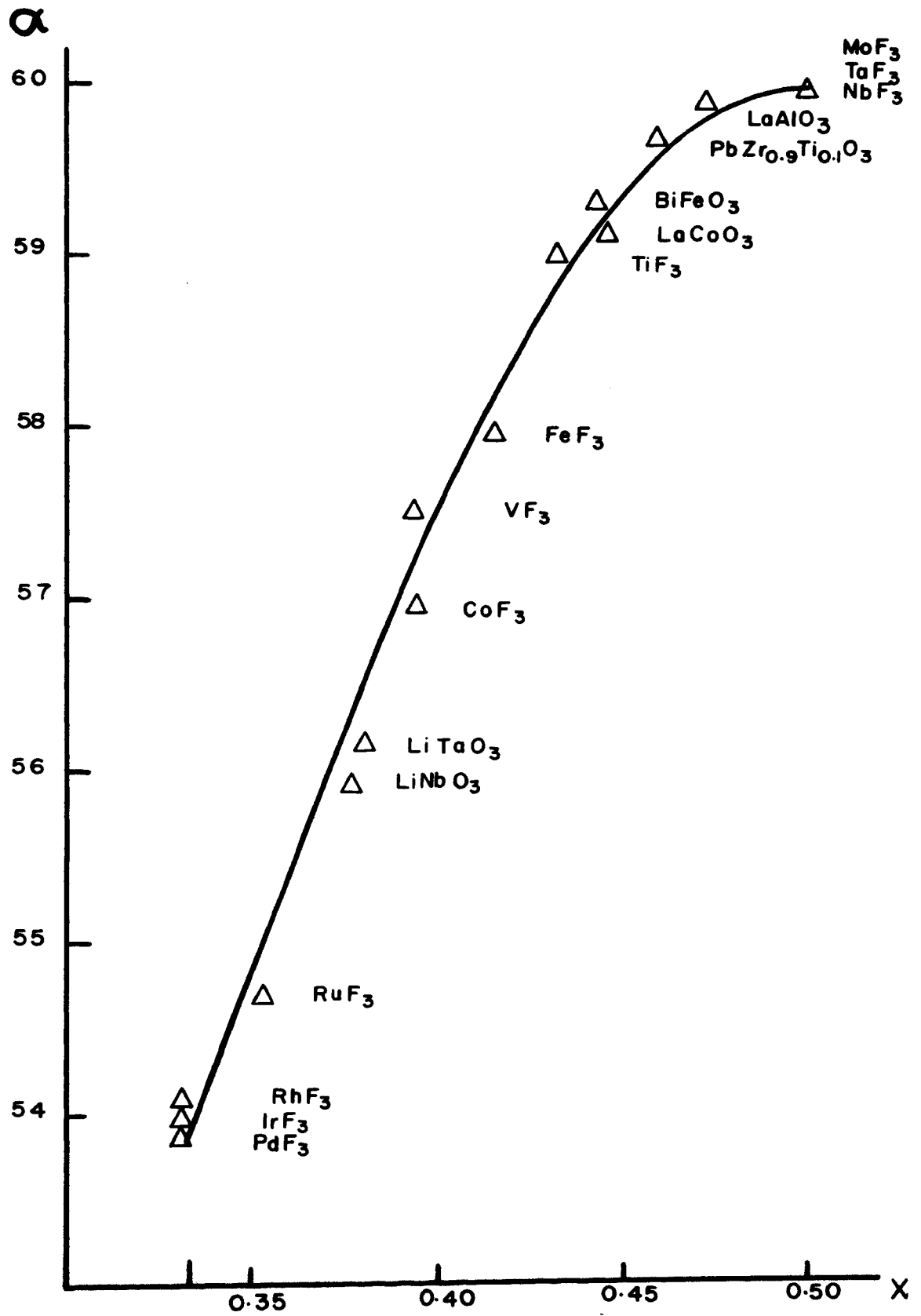Figure 13. Rhombohedral angle dependence
of the octahedral position parameter.

Figure 13

compounds, the metal atoms are in special positions given by the $R\bar{3}c$ space group.

However, in the isostructural series, $BiFeO_3$;[21] $PbZr_{0.9}Ti_{0.1}O_3$;[22] $LiTaO_3$;[29] $LiNbO_3$,[28] the metal atoms are shifted along the hexagonal axis from the sites $\underline{a}$ and $\underline{b}$. The symmetry is therefore reduced and the space group becomes the non-centrosymmetric $R3c$ space group. In this series the oxygen framework is more distorted from the idealized model due to the heavy atom shift. Nevertheless, the spread of the oxygen distances around the average is still small enough to consider these octahedra as regular to a first approximation. In other words, this framework can be considered as derived with a small systematic displacement of oxygen from the ideal model of higher symmetry.

Table III lists the different values of ϕ, x, and c/a for these perovskite-like compounds. The experimental values reported from the preceding series are in excellent agreement with those obtained from this theoretical relationship.

E. **Structural Phase Transition in Perovskite-type Crystals**

1. **Correlation with the trigonal rotation.**

a. **Superstructure reflection as in $LaAlO_3$.** From equation (1), the structure amplitude for superstructure reflections can be expressed by:

$$\left| F_{(\vec{H})} \right| \simeq \left| \sum_i f_i(\vec{H}) \, \Delta_i \, e^{\theta_i} \right|$$

with $\theta_i = 2\pi \vec{H}\vec{\delta}_i$. The vector $\vec{\delta}_i$ represents the small systematic displacement from the higher symmetry form.

The relation is valid only when Δ_i is small and can be applied only to reflections of low indices. The expression can be made more accurate by introducing further approximations for $\cos\Delta_i$ and $\sin\Delta_i$, bringing in terms in $|F|$ involving higher power of Δ_i, but this makes its application difficult.

If the superstructure reflections are only due to one type of atom, then, as a first approximation, $\left| F_{(H)} \right|$ is proportional to $|\vec{\delta}|$. For a trigonal distortion, as in BiFeO$_3$, $\vec{\delta}_i$ can be represented by the matrix $\begin{vmatrix} u \\ w \\ o \end{vmatrix}$. The oxygen positions are then defined by the matrix:

$$\pm[3]^i \begin{bmatrix} 1/2 + u \\ w \\ 1/4 \end{bmatrix} + \vec{R}_+ \quad (i = 1,2,3) \tag{20}$$

We have shown that the displacement parameter u is directly associated with the trigonal rotation. In all the compounds examined, the octahedra can be viewed as rigid, almost undistorted, units. Then, the magnitude of the parameter of distortion, w, is of second order compared to u. In the ideal case, as in LaAlO$_3$, $w = 0$, and the

symmetry is exactly $R\bar{3}c$. During the continuous transformation from the perovskite configuration to the hexagonal close-packed configuration, the parameter of rotation u varies from the value 0 to 1/6.

  b. Correlation. If u, the parameter of trigonal rotation is between 0 and 1/6, the superstructure reflection occurs when $\ell = 2n + 1$.($R\bar{3}c$, hexagonal set). Its absolute value can be expressed as a function of only one parameter, $x = 1/2 - u$.

$$F_{(hk\ell = 2n + 1)} = f_{(\vec{H})} A_{(x)}$$

The neutron form factor $f_{(\vec{H})}$ is independent of the diffusion factor $\vec{H}$.

$$A_{(x)} = \{\sin \pi [(h-k)x + \ell/2] \sin \pi i x$$

$$+ \sin \pi[(k-i)x + \ell/2] \sin \pi hx$$

$$+ \sin \pi[(i-h)x + \ell/2] \sin \pi kx \} \quad (21)$$

From equations (10) and (11) we can relate x to the trigonal rotation ω.

$$x = 1/2 - \frac{\tan \omega}{2 \sqrt{3}} \quad (22)$$

Consequently, in a structure with an octahedral framework of regular octahedra sharing corners and able to rotate without distortion, as in $LaAlO_3$, the amplitude of the resulting superstructure reflections is directly related to the trigonal rotation ω.

A specific superstructure reflection $F_{(\omega)}$ lies between the values,

$$F_{(o)} = 0 \quad \text{and} \quad F_{(\omega= \frac{\pi}{6})} = f_{(\vec{H})} \ A_{(x=1/3)}$$

From equations (1) and (22) in the case of small rotation, a superstructure reflection, $I_s(\omega)$, can be approximated as a first order by the direct relation:

$$I_s(\omega) \simeq \alpha\omega^2$$

where α is a coefficient of proportionality depending only on the Bragg angle. Fig. 14 shows the theoretical curve $I_s = |F_{(\omega)}|^2$ computed from equations (21) and (22) for different values of ω of the specific reflection [113].

2. <u>Theory of the phase transition</u>. The structural phase transitions in the ABO_3 perovskite-type compounds involving rotations of the BO_6 octahedra have been the subject of a number of recent investigations.[38,40,45,46] These phase transitions are due to the condensation of
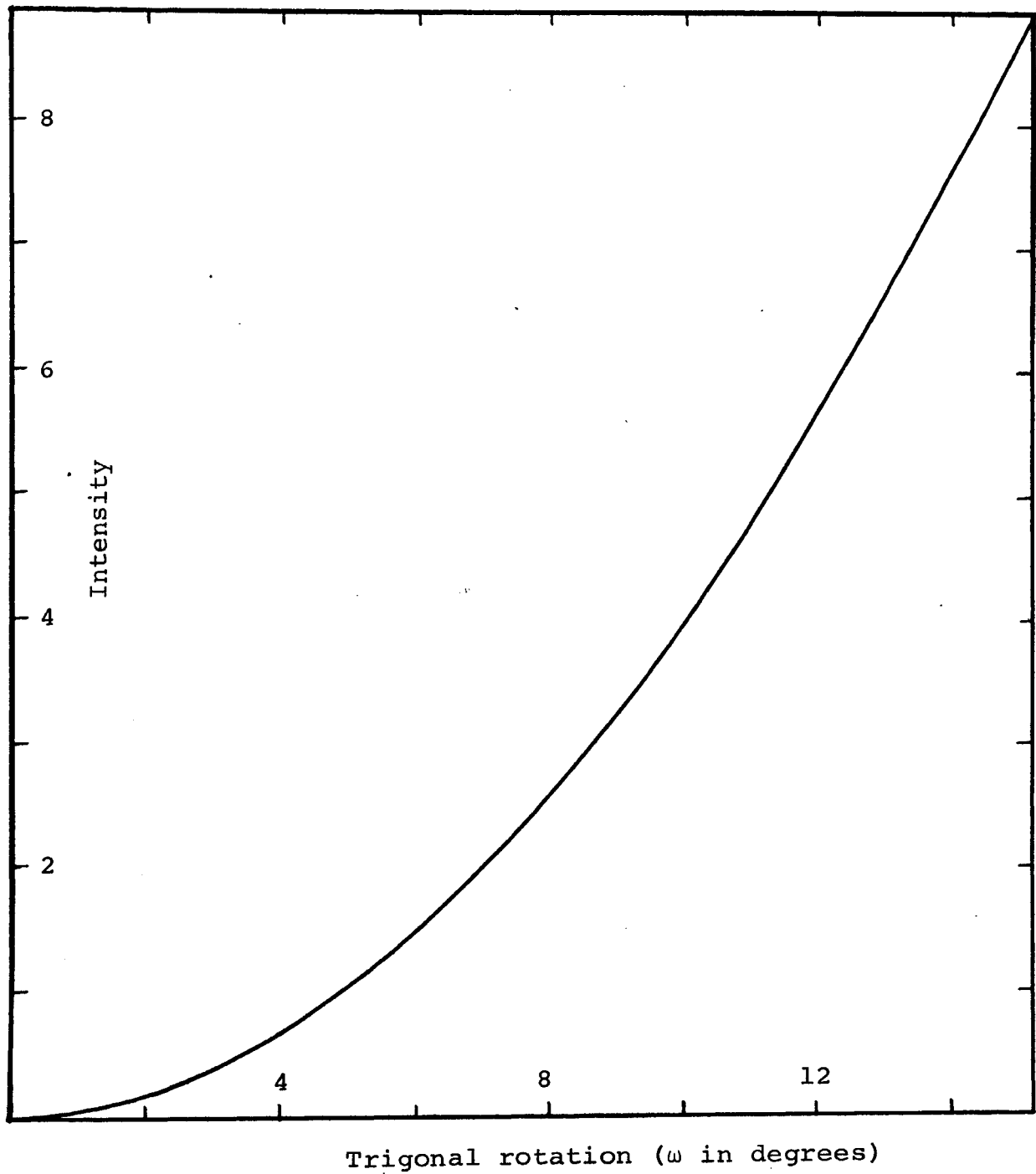
Figure 14. Theoretical variation of the superstructure in-
tensity of the reflection [113] as a function of
the trigonal rotation of BO_6 octahedra.

linear combinations of the triply Γ_{25} modes at the R

corner of the Brillouin zone.[46] So far, phase transitions

of this type are known to occur in $SrTiO_3$, $KMnF_3$, and

$LaAlO_3$ at about 105, 184 and 806°K, respectively. A

model Hamiltonian has recently been constructed in order

to explain these displacive structural phase transitions.

In this model, the rotation of oxygen octahedra are de-

scribed in terms of axial vectors associated with the

localized displacement field.

For a trigonal distortion as in $LaAlO_3$ the primitive

unit cell is enlarged and the Brillouin zone is corres-

pondingly reduced. In this particular case, the model of

Hamiltonian is described [49] only by three degrees of

freedom. The displacements of the oxygen octahedra are

coupled to the static strains, and this anharmonic inter-

action can be approximated by a simple form containing

only two anharmonic force constants.

The resulting temperature dependencies of the dis-

tortion angle and of the frequencies of the soft Γ_{25}

optical modes have been calculated by Pytte.[49]

Fig. 15 shows the angle of rotation in $LaAlO_3$, nor-

malized to its value at T = 0, as a function of reduced

temperature. Experimental points obtained by E.P.R. and

neutron diffraction by Muller, et. al.,[38] are in excellent

agreement with the theoretical curve calculated from the

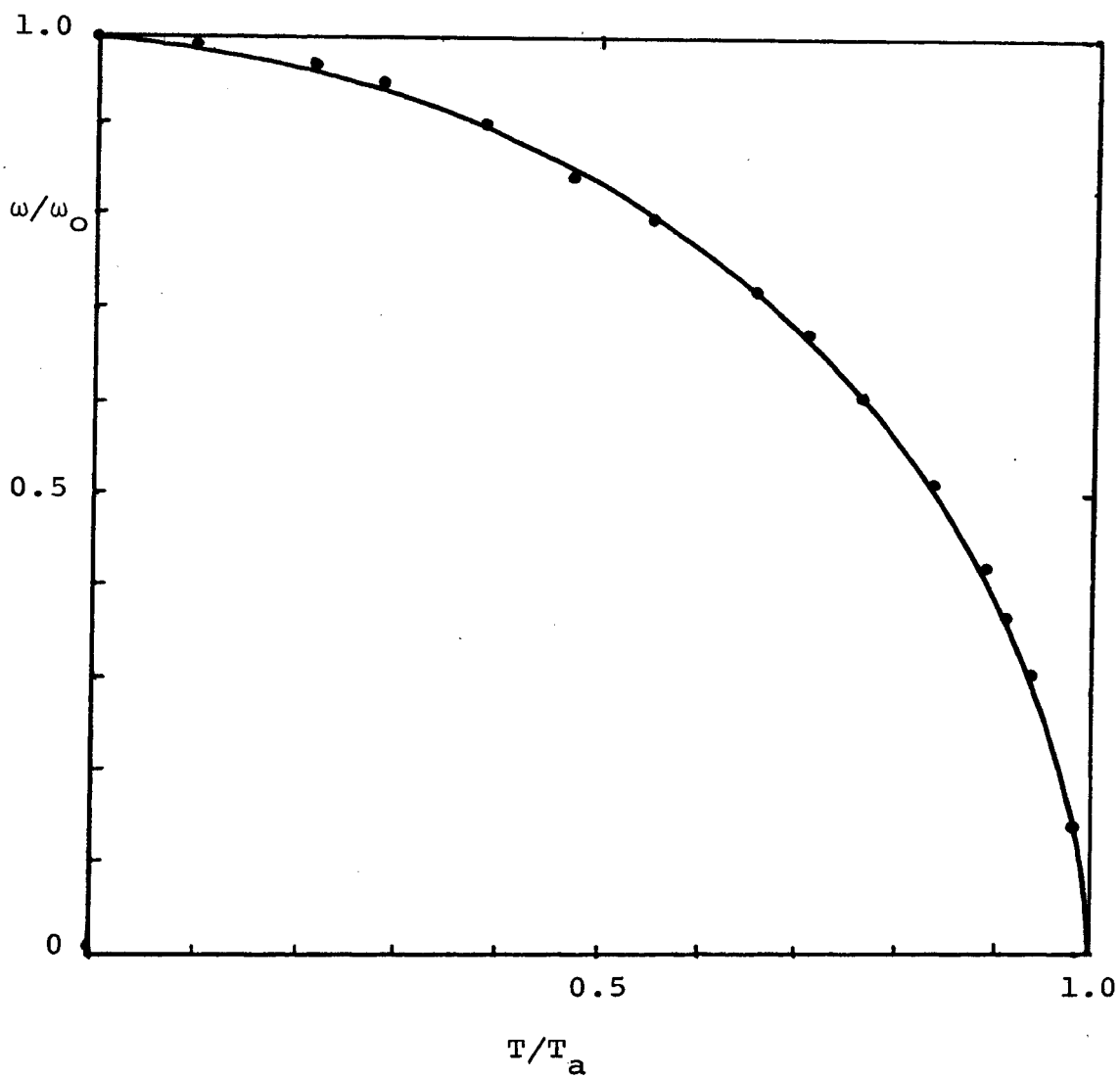model of Hamiltonian. The fact that one mode is involved

Figure 15.   Angle of rotation in LaAlO$_3$ normalized to its

value at T = 0 as a function of reduced

temperature calculated from the theory.

by the vibrations of oxygen only, suggests the use of neutron or x-ray scattering to investigate the transition.

3. Analogy with theoretical results of $LaAlO_3$.

Experimental and theoretical results in $LaAlO_3$ have shown that when the temperature increases the trigonal rotation ω decreases. Thus, the corresponding amplitude of a super-structure reflection only due to this trigonal rotation should also decrease uniformly. Such a variation was observed by Platkhy[45] with x-ray diffraction on the [711] superstructure reflection.

Similar behavior obtained with neutron diffraction on $PbZr_{0.9}Ti_{0.1}O_3$ suggests strongly an analogy with the $LaAlO_3$ results.

Fig. 16 shows this temperature dependence of neutron diffraction intensity of the specific superstructure reflection [113]. These neutron diffraction data were taken with a slow count rate at O.R.N.L. research reactor on pure polycrystalline materials of $Pb(Zr_{0.9}Ti_{0.1})O_3$. The intensity of the superstructure reflection decreases uniformly with rising temperature and disappears at 110°C below the ferroelectric Curie temperature (250°C). Between 110°C and 250°C, the cell is reduced to a mono-atomic unit cell with all oxygens shifted equivalently. The difference between these two phases can then be described in terms of oxygen shifts, as is shown in Fig. 17. Away from the transition, the temperature dependence of the
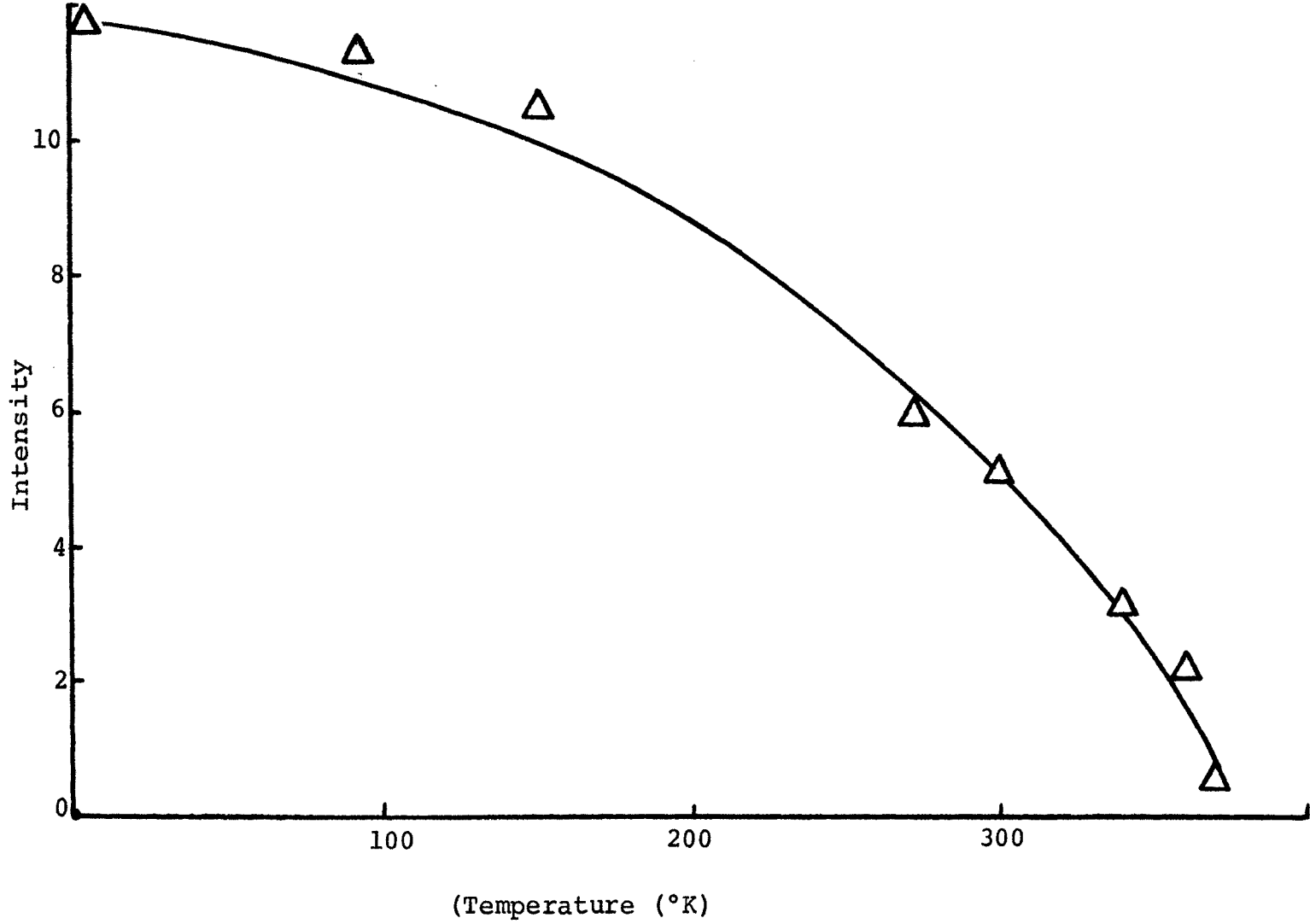
Figure 16. Temperature dependence of the intensity [113]; Neutron powder data on Pb $Zr_{0.9}$ $Ti_{0.1}$ O_3 .

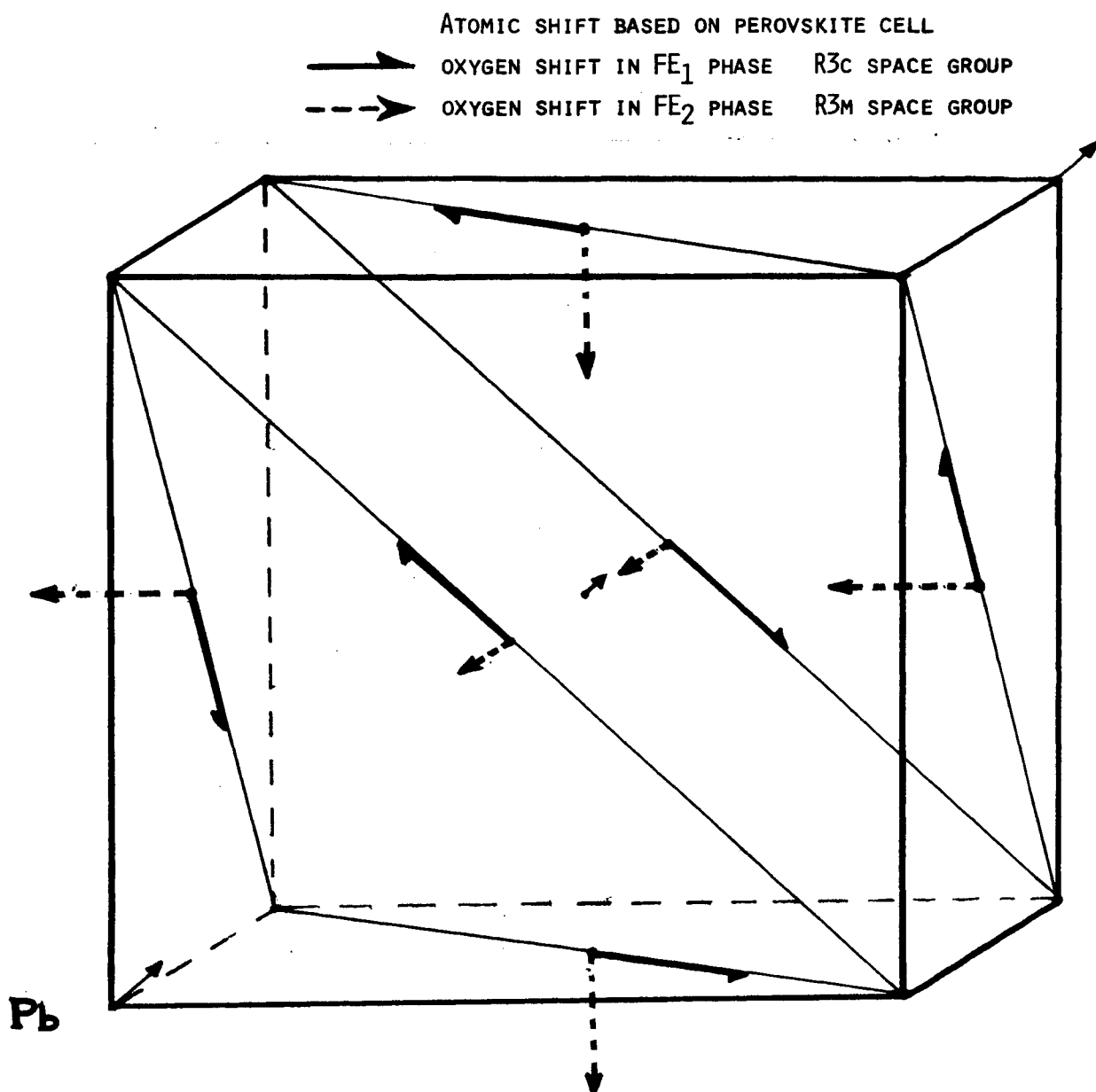ATOMIC SHIFT BASED ON PEROVSKITE CELL

⟶ OXYGEN SHIFT IN FE_1 PHASE   R3c SPACE GROUP

⇢ OXYGEN SHIFT IN FE_2 PHASE   R3M SPACE GROUP

Pb

Figure 17. Atomic shift in Pb $Zr_{0.9}$ $Ti_{0.1}$ O_3.

STRUCTURE OF $PB(ZR_{0.58}TI_{0.42})O_3$ IN FE_2 PHASE

SPACE GROUP R3M $a_R = 4.07$ Å

$\alpha = 89°39'$

P_B (δδδ), WITH δ = 0.552

ZR-TI (εεε), WITH ε = 0.038

O (γ○○), (○γ○) AND (○○γ), WITH γ= 0.558

intensity of the superstructure reflection [113] can be considered as mainly due to the trigonal rotation ω.

From our crystallographic data[23] $\omega = 8°$ at room temperature for $PbZr_{0.9}Ti_{0.1}O_3$. The room temperature experimental value of the superstructure reflection intensity [113] has been normalized with the theoretical intensity value calculated for $\omega = 8°$, and then the corresponding temperature dependence of the trigonal rotation, ω , was calculated.

The resulting curve of ω versus temperature is plotted in Fig. 18. The agreement with the theoretical results of Pytte for $LaAlO_3$ is very close. The similarity of the temperature behavior and the phase transitions of $LaAlO_3$ and $Pb(Zr_{0.9}Ti_{0.1})O_3$ is obvious.

Although the results are consistent with the existence of a "soft" mode, $Pb(Zr_{0.9}Ti_{0.1})O_3$ is the first reported material exhibiting such a mode below its ferroelectric Curie point.
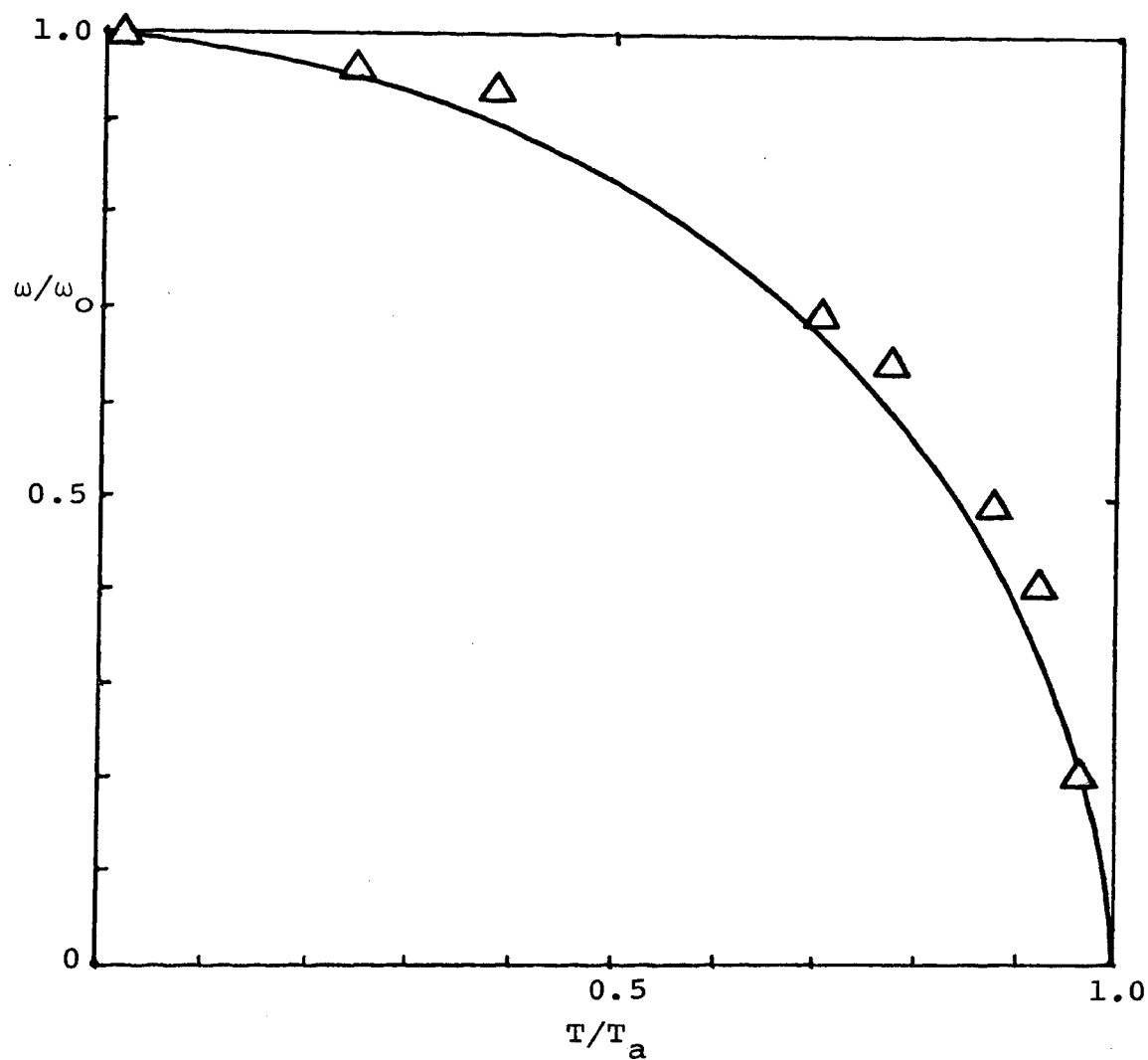
Figure 18. Trigonal rotation ω as a function of the
temperature in reduced coordinates; Neutron pow-
der data on Pb Zr$_{0.9}$ Ti$_{0.1}$ O$_3$. (△ , observed
data; solid line, theoretical curve from Pytte.)

IV. SUMMARY AND CONCLUSIONS

It is clear from Table IV that the trifluoride series can be referred to the perovskite-type series by considering both as based on the same framework of regular octahedra, sharing corners and topologically capable of rotation around their three-fold axes without appreciable distortion.

Results from theoretical considerations are in agreement with experimental data. Several important conclusions can be drawn from this study:

To a first approximation, BO_6 octahedra behave as homogeneous isotropic units in all of these compounds.
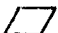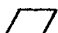
The high symmetry form of a regular octahedral framework able to rotate around their three-fold axes is in the $R\bar{3}c$ space group. This framework is an intermediary between the hexagonal close-packed and the perovskite configuration.

The trigonal BO_6 rotation is independent of the B cation shift in the ferroelectric compounds. This shift involves a distortion of the octahedron which is negligible compared to its tilt.

The atomic positions of the octahedral framework and the bond angle MOM can be predicted by the magnitude of the c/a ratio or the pseudocubic angle. These parameters are easily measurable with sufficient accuracy by x-ray

TABLE IV

OCTAHEDRA COORDINATES

Octahedra Atoms	Octahedra X Coordinate	site b z_b	site a z_a	Compounds
Ideal	2/3	▱	▱	Hexagonal - Close-packed
	1/2	▱	▱	Octahedra in perovskite configuration
	1/2	▱	0	Cubic-face-centered
	x	▱	▱	Intermediate Model $R\bar{3}c$ space group: $0 < |\omega|\ \frac{\pi}{6}$
F	2/3	0	▱	RhF_3, PdF_3, IrF_3
	1/2	0	▱	NbF_3, MoF_3, TaF_3
	x	0	▱	VF_3, FeF_3, CoF_3, RuF_3, TiF_3
O	1/2	0	▱	ReO_3
	1/2	0	1/4	ABO_3 ideal perovskite
	x	0	1/4	$LaAlO_3$, $LaCoO_3$ in $R\bar{3}c$ space group
	x	ε_b	$1/4 + \varepsilon_a$	$LiNbO_3$, $LiTaO_3$, $BiFeO_3$, $PbZr_{0.9}Ti_{0.1}O_3$ in R3c space group (Shift ε_b, ε_a)

techniques. Hence, the established relationship is a powerful tool for structure determinations.

The macroscopic thermal expansion is the sum of parts due to the change of the mean edge of the octahedron and the change of octahedron tilt. When changes of tilt are allowed by symmetry, their contribution to the macroscopic expansion is considerably greater than that of changes of octahedron size. Hence, from the change of the c/a ratio as a function of the temperature, it is possible to predict the corresponding tilt of the anion octahedra.

If the rotation of the octahedra versus the temperature is known, as in $LaAlO_3$, it is possible to predict the expansion parameter.

For the isomorphous series, $BiFeO_3$, $Pb(Zr_{0.9}Ti_{0.1})O_3$, $LiTaO_3$, $LiNbO_3$, the B cation shift is directly related with the Curie temperature and the spontaneous polarization by the equation (3). From our crystallographic data reported in 22, the A cation shift seems to be correlated linearly with the B cation shift. In such a case, using only the knowledge of the cell parameters and the Curie temperature, it is possible to predict the atomic structure of these compounds and give a good approximation of the spontaneous polarization.

In this kind of structure, the resulting superstructure reflections are only due to the anions. We have shown in an idealized model that the intensity of the super-

structure reflections are directly related with only one parameter, the trigonal octahedra rotation ω. A method is developed to calculate ω versus temperature from the temperature dependence of a specific superstructure line's reflection intensity.

The curve of ω versus temperature derived for $Pb(Zr_{0.9}Ti_{0.1})O_3$ presents a very close similarity with the theoretical temperature dependence of ω calculated for $LaAlO_3$. This suggests strongly the existence of a "soft" mode for $Pb(Zr_{0.9}Ti_{0.1})O_3$ below its ferroelectric Curie point, with an unstable phonon mode at the ($\frac{1}{2}\frac{1}{2}\frac{1}{2}$) point at the Brillouin zone corner associated with the trigonal BO_6 rotation.

Applications to structures other than those cited in this work should also be considered.

V. BIBLIOGRAPHY

1. Megaw, H.D., Ferroelectricity in Crystals, Methuen, London, pp. 83-123 (1957).

2. Fatuzzo, E., Ferroelectricity, Oxford Press, pp. 5-102 (1967).

3. Shirane, G., Ferroelectric Crystals, Pergamon Press, pp. 108-383 (1962).

4. Roth, R., Nat. Bur. Standards, 58, 75 (1957).

5. Roberts, S., Phys. Rev., 81, 865 (1951).

6. Goodenough, J., Phys. Rev., 100, 564 (1955).

7. Granovskii, G., Sov. Phys. Crist., 7, 484 (1963).

8. Keith, L. and R. Roy, Am. Miner., 39, 1-23 (1954).

9. Megaw, H.D., Act. Cryst., 7, 197 (1954).

10. Fatuzzo, E., Ferroelectricity, Oxford Press, pp. 105-269 (1967).

11. Megaw, H.D., Ferroelectricity in Crystals, Mathuen, London, 14 (1957).

12. Kanzig, W., Ferroelectrics and Antiferroelectrics, Solid State Reprints, Academic Press, N.Y., pp. 5-6 (1957).

13. Kittel, C., Phys. Rev., 82, 729 (1951).

14. Shirane, G., R. Pepinsky and B. Frazer, Phys. Rev., 84, 476 (1951).

15. Jona, F., G. Shirane, F. Mazzi and R. Pepinsky, Phys. Rev., 105, 849 (1957).

16. Barnett, H., J. Appl. Phys., 33, 1606 (1962).

17. Berlincourt, D., IEEE Trans. on Sonics and Ultrasonics, SU13, 116 (1966).

18. Berlincourt, D., H. Krueger and B. Jaffe, Phys. Chem. Solids, 25, 659 (1964).

19. Megaw, H.D., Ferroelectricity in Crystals, Methuen, London, pp. 124-134 (1957).

20. de Rango, C., G. Tsoucaris and C. Zelwer, Acta. Cryst., 20, 590 (1966).

21. Michel, C., J.M. Moreau, G. Achenbach, R. Gerson, and W.J. James, Solid State Comm., 7, 701 (1969).

22. Michel, C., J.M. Moreau, G. Achenbach, R. Gerson, and W.J. James, Solid State Comm., 7, 865 (1969).

23. Moreau, J.M., C. Michel, R. Gerson and W.J. James, to be published, Acta. Cryst. (1969).

24. Michel, C., J.M. Moreau, W.J. James, to be published, Acta. Cryst. (1970).

25. Tomashpolskii, Y., Y. Venevtsev, and G. Zhdanov, Sov. Phys. Cryst., 12, 209 (1967).

26. Plakhty, V., F. Maltsev and D. Kaminker, Bull. Acad. Sci. U.S.S.R., Phys. Ser., 28, 350 (1964).

27. Tomashpolskii, Y., Y. Kenevtsev and G. Zhdanov, Sov. Phys. Cryst., 9, 715 (1967).

28. Abrahams, S., W. Hamilton and J. Reddy, J. Phys. Chem. Solids, 27, 1013 (1966).

29. Abrahams, S. and J. Bernstein, J. Phys. Chem. Solids, 28, 1685 (1967).

30. Bailey, J.E., Thesis Bristol (1952).

31. Megaw, H.D., Acta. Cryst., A 24, 583 (1968).

32. Hepworth, M., K. Jack, R. Peacock and G. Westland, Acta. Cryst., 10, 63 (1957).

33. Jack, K., and V. Gutmann, Acta. Cryst., 4, 266 (1951).

34. Gutmann, V. and K. Jack, Acta. Cryst., 4, 244 (1951).

35. Kupriyanov, M. and V. Filipev, Sov. Phys. Cryst., 8, 278 (1963).

36. Megaw, H.D., Acta. Cryst., B 24, 169 (1968).

37. Abrahams, S.C., S.K. Kurtz and P.B. Jamieson, Phys. Rev., 172, 551 (1968).

38. Müller , K.A., W. Berlinger, and F. Waldner, Phys. Rev., 21, 814 (1968).

39. Fleury, A., J.F. Scott and J.M. Worlock, Phys. Rev. Letters, 21, 16 (1968).

40. Müller, K.A., F. Brun, B. Derighetti, J.F. Drumheller and F. Waldner, Phys. Letters, 9, 223 (1964).

41. Cochran, W. and A. Zia, Phys. Status Solidi., 25, 273 (1968).

42. Megaw, H.D., Acta. Cryst., A 24, 589 (1968).

43. Menyuk, N., K. Dwight and P.M. Raccah, J. Phys. Chem. Solids, 28, 549 (1967).

44. Cochran, W. and A. Zia, Phys. Status Solidi., $\underline{25}$, 273 (1968).

45. Platkhy, V. and W. Cochran, Phys. Status Solidi., $\underline{29}$, K81 (1968).

46. Axe, J.D., G. Shirane and K.A. Müller, Bull. Am. Phys. Soc., $\underline{14}$, 61 (1969). Phys. Rev., $\underline{183}$, 820 (1969).

47. Thomas, H. and K.A. Müller, Phys. Rev. Letters, $\underline{21}$, 1256 (1968).

48. Cochran, W., Rep. Progr. Phys., $\underline{26}$ (1963).

49. Pytte, E. and F. Feder, Phys. Rev., $\underline{187}$, 1077 (1969).

VI. VITA

Christian Michel was born in Tunis, Tunisia on October 25, 1939. He received a baccalaoureate degree from Lycee Champollion, Grenoble (France) in 1957 and entered the University of Grenoble (France), receiving a Licence in Physics and Chemistry in 1954, a diplom of Etude Appronfondie in 1965, and the degree of Doctor in Speciality (3^e cycle) in magnetism and solid state physics in June, 1967. In October of 1967 he enrolled in the University of Missouri at Rolla and has held a post-doctoral research fellowship sponsored by the Atomic Energy Commission.